REVIEW ARTICLE

Learning from biological attachment devices: applications of bioinspired reversible adhesive methods in robotics

Kun XU, Peijin ZI, Xilun DING (✉)

School of Mechanical Engineering and Automation, Beihang University, Beijing 100191, China
✉ *Corresponding author. E-mail: xlding@buaa.edu.cn (Xilun DING)*

ABSTRACT Many organisms have attachment organs with excellent functions, such as adhesion, clinging, and grasping, as a result of biological evolution to adapt to complex living environments. From nanoscale to macroscale, each type of adhesive organ has its own underlying mechanisms. Many biological adhesive mechanisms have been studied and can be incorporated into robot designs. This paper presents a systematic review of reversible biological adhesive methods and the bioinspired attachment devices that can be used in robotics. The study discussed how biological adhesive methods, such as dry adhesion, wet adhesion, mechanical adhesion, and sub-ambient pressure adhesion, progress in research. The morphology of typical adhesive organs, as well as the corresponding attachment models, is highlighted. The current state of bioinspired attachment device design and fabrication is discussed. Then, the design principles of attachment devices are summarized in this article. The following section provides a systematic overview of climbing robots with bioinspired attachment devices. Finally, the current challenges and opportunities in bioinspired attachment research in robotics are discussed.

KEYWORDS adhesion, bioinspired attachment, biomimetic gripper, climbing robot

1 Introduction

In nature, animals with varying body weight, such as geckos, octopuses, and beetles, can attach or move freely on walls or inclined surfaces with a wide range of roughness and materials. These organisms have various efficient attachment organs (e.g., seta of gecko [1,2], sucker of octopus [3], and claws of insects [4,5]) with unique morphologies and special biological functions for clinging to contacted surfaces [6,7]. The types of reversible attachment can be classified into four categories based on the biological adhesion mechanisms, as shown in Fig. 1.

(i) Dry adhesion is based on van der Waals force between the setae and the attached substrate and is found in gecko [1,2] and spider [8–10];

(ii) Wet adhesion is based on a unique interaction among the adhesive pads, mucus, and the attached surfaces and is found in some amphibians, arthropod, and molluscs [11];

(iii) Mechanical adhesion is based on the adhesive mechanisms of biological spines, snaps, clamps, and claws and is exploited by some arthropod, birds, reptiles, and other animals [6];

(iv) Sub-ambient pressure is employed by suckers of some molluscs and fish to produce adhesion [3,12].

Attachment devices for robots require dependable and compliant adhesive techniques that can help robots to complete some dangerous or complex tasks (e.g., building maintenance, field reconnaissance and rescue, bridge inspection, space station maintenance, and planet and asteroid exploration). These potential application scenarios pose technical challenges for robot attachment devices. Industrial adhesion methods include negative pressure [13,14], aerodynamic force [15], and magnetic adhesion [16] used in robotics, particularly in the field of climbing robots from 1960s. On the contrary, these attachment devices based on traditional artificial adhesion technology have some drawbacks, as follows:

(i) Many of them often consume a remarkably amount of energy, whether moving or stationary, and require assistance from an external power energy supply [17], reducing the robot system's autonomous motion performance;
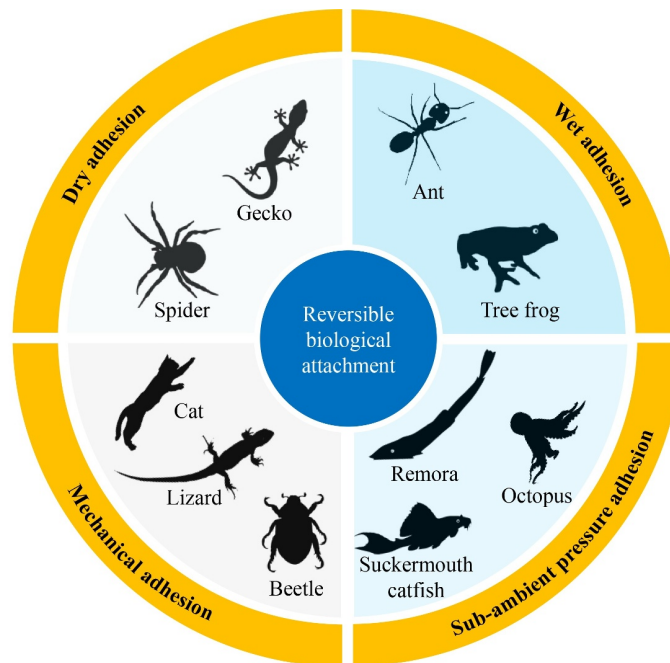
Fig. 1   Four categories of reversible biological attachment methods and typical animals of each type.

(ii) Many of them produce noise even when stationary [17,18];

(iii) They are unable to adapt to an environment with time-varying constraints and complicated topography due to lack of adequate compliance, adhesion, and robustness [19];

(iv) The efficiency and the ratio between practical adhesion and deadweight of the attachment devices remain lower than those of animals.

(v) Environmental medium and surface materials can readily limit their application. For example, negative pressure adsorption cannot be applied in space environment, and magnetic adsorption can only be used for attachment on ferromagnetic surfaces.

A number of adhesion strategies have been discovered by investigating attachment of creatures during parasitism, hunting, climbing, and copulation, thereby motivating researchers to build bionic materials and technologies to improve the attachment performance of robots. In recent years, researchers have attempted to mimic biological adhesive organs to construct artificial attachment devices, as well as to research the design and manufacturing technology of climbing robots. A significant variety of bioinspired adhesives [20,21], suckers [12,22], and microspines [18,23] is conceived and manufactured to improve robot attachment performance. Many bioinspired climbing robots and manipulators have impressive abilities [24–27]. Bioinspired attachment systems are exploding and hold great promise for robotics applications.

In this study, we review the current state-of-the-art approach in reversible bioinspired attachment systems and its applications in robotics. Sections 2–5 present the four categories of bioinspired adhesive technologies studied, each with matching biological organs, mechanisms, bionic integration, and applications in robotics. The current state of the bioinspired attachment methods in the application of bionic robotic grippers and climbing robots is discussed in detail. Section 6 outlines the design methodologies of bionic attachment devices, integration methods of bioinspired climbing robots, and present challenges and prospects of the bionic attachment.

2   Dry adhesion

Dry adhesion is an interaction primarily caused by van der Waals forces and friction, and some animals in nature can use dry adhesion to rapidly switch between attachment and detachment to complete the climbing motion [1,2,28]. Although studies on geckos' attachment and movement capabilities date back over two thousand years, its underlying mechanism based on van der Waals force was never proven until 2000 [29]. A number of bioinspired dry adhesives have been developed, following the discovery of the gecko attachment mechanism. In some performance indices, such as adhesion, artificial adhesives can match or even outperform biological adhesives. Some of them have been used in climbing robots and grippers. The morphology and potential mechanisms of biological dry adhesive organs, as well as the application of bioinspired dry adhesives to climbing robots and grippers, are discussed in this section.

2.1 Biological devices and mechanism

Van der Waals forces are the weakest of all intermolecular forces, while being the most widespread. The van der Waals force attracts electroneutral atoms if their distance is equal to or higher than their size [30]. The force per area F_a due to van der Waals force between two planar surfaces is estimated using the following equation:

$$F_a = \frac{A}{6\pi D^3},\qquad (1)$$

where A represents the Hamaker constant, a function of the volume and polarizability of the molecules involved, it is generally scaled between 4×10^{-15} and 4×10^{-20}. D represents the separation distance between the two surfaces. The Johnson–Kendall–Roberts model and elastic beam theory are frequently utilized to characterize spatula-substrate contact [31,32].

According to the van der Waals force principle, the dry adhesive qualities of gecko setae are mostly related to the size and shape of their terminals, with surface chemistry having little effect [29]. The remarkable adhesive ability of gecko's pad is primarily due to the following features.

(i) Hierarchical structure. Geckos and spiders have adhesive pads that are densely covered with tree-like hierarchical setae, which can increase their compliance and real contact area, as shown in Fig. 2 [33]. The lamella on the adhesive pad has a three-level hierarchical structure that includes setae, branches, and spatulae. The actual adhesion between the substrate and a single seta with a spatulae terminal can be nearly 200 mN [1]. If the number of spatulae in each seta is assumed to be 100−1000, then the equivalent separation distance in Eq. (1) is 0.38−0.81 nm [33]. A tokay gecko (*Gekko gecko*) can resist 20.1 N of pull force by exploiting 227 mm² adhesive area in its front feet theoretically [34]. The spatulae are composed of β-keratin, a stiff natural material, which has a Young's modulus of approximately 1.4 GPa [35]. At the terminal of the hierarchical structure, the spatula pads are merely approximately 5 nm thick, thereby allowing them to be feasibly absorbed on a solid substrate [36].

(ii) Special shape of seta. Setae are virtually oblique and curved in shape, and they are invariably orientated to the distal end of the limb, as shown in Fig. 2(d) [33]. When the limbs are attached to the surface and move relative to the body, these setae are not flattened and clumped, but are fixed under tension. Furthermore, the skewness of the setae improves their flexibility in the normal direction and increases their surface compliance [37].

(iii) Self-cleaning. Biological adhesives used for attachment in various scenarios must have mechanisms for maintaining cleanliness [37]. This phenomenon has been described as dirt particles among the setae being removed after the gecko walked few gait cycles on a clean surface [38]. According to the research, dirty particles prefer to stick to the wall rather than spatulae [38]. Niewiarowski et al. [39,40] discovered that gecko setae generate sufficient inertial force to dislodge dirt particles between spatulae during sudden detachment from the substrate. The self-cleaning ability of gecko seta is aided by their non-tacky materials with low surface energy, macroscopic movement, and specific tip shape [41].

(iv) Directional adhesion. Climbing movement necessitates a strong adhesion and rapid peeling with low consumption [42]. Geckos can separate their feet from the substrate in 15 ms with nearly little disengaging forces [43]. Gravish et al. [43] discovered that the ideal peeling angle of the setae is 130° between substrates given the negative returning elastic energy and the effort of detachment in this direction. Chen et al. [37] used the beam model to determine the peeling force of a single spatula, and the force is approximately 10 times more in 30° than in 90° of peeling angle in theory.

2.2 Dry adhesives and their applications in robotics

Bio-inspiration provides a common design paradigm for artificial adhesives that may be widely employed in robotics. We focus on classification of bioinspired dry adhesives, and their applications in robotics are discussed in this work. References [44,45] show the state of art information on the features and manufacturing processes of various types of dry adhesives. A growing number of climbing robots and robotic gripper attachment devices use dry adhesives for attachment due to their popularity. Attachment devices of bioinspired climbing robots that use dry adhesion can be classified into three groups based on their locomotion mode: leg, wheel-leg (wheg), and track. However, due to limits in self-cleaning, wear resistance, and compliance for rough surfaces of dry adhesives, these robots cannot function on dusty and rough surfaces yet.

2.2.1 Dry adhesives

Inspired by gecko setae, three dry adhesive fibril features are proposed: (i) As many contacting fibrils as possible should be placed in each unit area, to boost adhesive strength via van der Waals forces; (ii) width–length ratio and material stiffness cause the elastic energy stored in the fibrils to be less than the adhesion work; (iii) fibrils should not be bound and agglomerated [46].

Many different types of single-level fibrillar structures have been created by molding polymers through nano indentations and nano porous filters that closely resemble gecko adhesive [47–52]. Contact geometry is an important factor in optimizing the adhesive property.
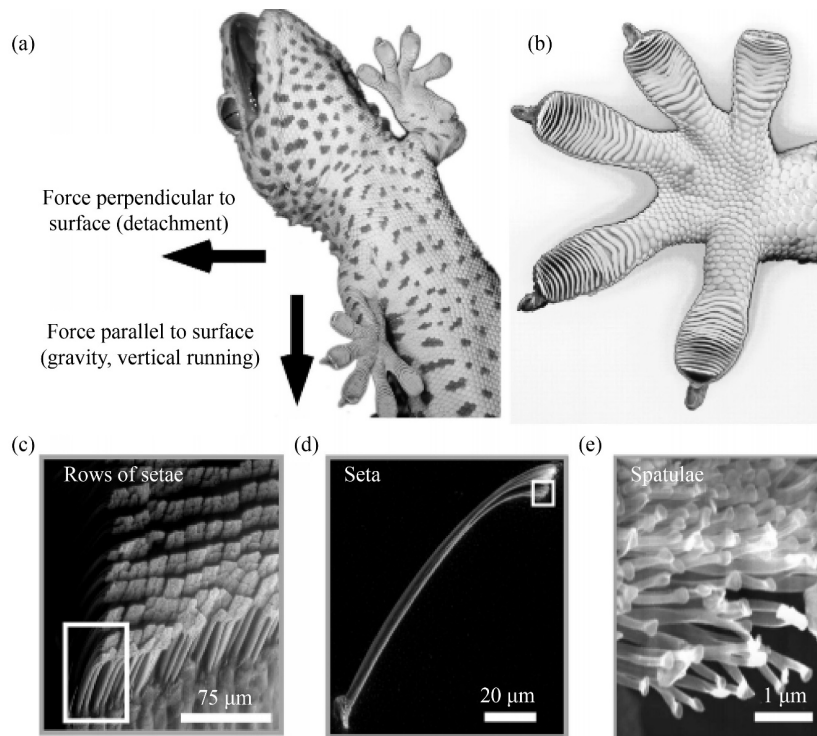
Fig. 2 Illustration of hierarchical structure of the gecko adhesive pad from macroscale to nanoscale: (a) ventral view of a tokay gecko (*Gekko gecko*), (b) foot, (c) setae, (d) single seta, and (e) arrays of spatular tips of a single seta. Reproduced with permission from Ref. [33] from Oxford University Press.

Figure 3 [24,53–58] shows a few of the dry adhesives that have been applied by robots. According to several studies, mushroom-shaped adhesive microstructure (MSAMS) fibrils exhibit stronger adhesive capability than planar, spherical, and spatulate fibrils, as well as higher hierarchical potential [59–61]. Furthermore, MSAMS fibrils have advantages in cracking resistance and surface defect reduction for avoiding stress concentration at the interface [62–64]. As a result, MSAMS are commonly employed in the design of artificial bioinspired dry adhesive surfaces. Many MSAMS adhesive pads, such as those shown in Figs. 3(a)–3(c) [53–55], have been used in robots.

The directional adhesion inspired by geckos is essential for adhesive application, allowing robots to engage and disengage from surfaces rapidly and efficiently [65]. Anisotropic microstructures, such as sloped and wedged structures shown in Figs. 3(d)–3(g) [24,56–58], can controllably and compliantly transition adhesives between strong adhesion and easy separation via shear movements [20,56,66]. Sloped or wedged structures are commonly employed in the design of controlled dry adhesives to provide anisotropic adhesion due to their flexural modulus, contact region, and detachment angle properties. Parness et al. [56] used dual exposure lithographic mold making process to make wedge-shaped dry adhesives with long lifetime. Wang et al. [67] achieved anisotropic adhesion on inclined MSAMS dry adhesive surfaces. Furthermore, asymmetric tips with various geometric shapes on sloped or vertical fibrils are possible methods for obtaining anisotropic dry adhesive surfaces [51,68,69]. These dry adhesives are perfect for robot attachment because they can be used in conjunction with movements of the mechanisms of robotic grippers or the toes of climbing robots to provide strong adhesion and quick release.

Greater adhesion can be acquired by developing hierarchical and refined setae [2]. Hierarchical designs can increase structural compliance on surfaces with varying degrees of roughness while maintaining adhesion strength [70]. Initially, in hierarchical fibrillar structures, smaller fibrils were simply attached to basic supporting fibrils to increase equivalent contact surface [71]. Many different types of hierarchical structures, such as MSAMS and sloping structures created by diverse manufacturing procedures, currently flourish [65]. However, current hierarchical dry adhesives are rarely used in robots due to their ease of wear and tip clustering.

Generally, fibrils made by silicon rubbers, such as polydimethylsiloxane (PDMS) and polyvinyl siloxane (PVS), are demold easily, hydrophobic, environmentally insensitive, and reusable. They also have advantages on self-cleaning property and low surface energy [44]. The MSAMS adhesive surfaces can be fabricated by demolding from the master mold, photolithography, and etching [65]. Two-photon lithography is a recent method,
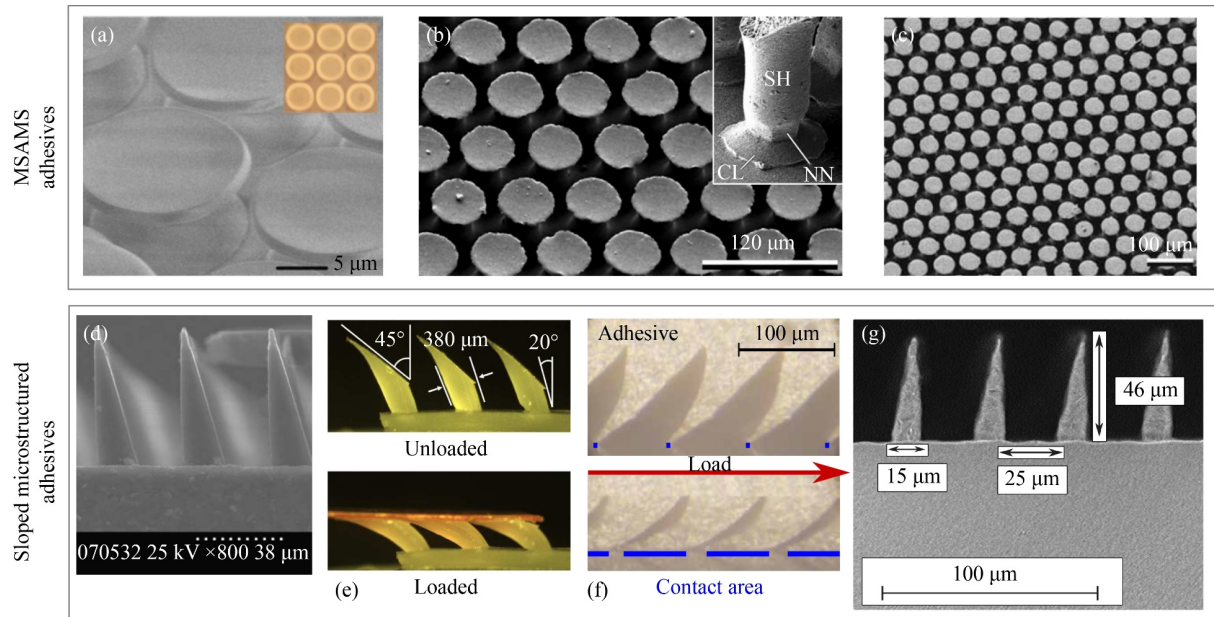
Fig. 3 Artificial adhesives used in robotics: (a) MSAMS adhesive used in TBCP-II, reproduced with permission from Ref. [53] from IOP Publishing, (b) MSAMS adhesive used in Mini-Whegs, reproduced with permission from Ref. [54] from IEEE, (c) MSAMS adhesive used in gecko robot_7, reproduced with permission from Ref. [55] from ACTA Press, (d) adhesives with wedged structure, reproduced with permission from Ref. [56] from Royal Society, (e) adhesives with wedged structure used in Stickybot, reproduced with permission from Ref. [24] from IEEE, (f) adhesives with wedged structure used in the space gripper, reproduced with permission from Ref. [57] from The American Association for the Advancement of Science, and (g) adhesives with wedged structure used in soft gripper, reproduced with permission from Ref. [58] from IEEE.

which allows high spatial control to generate micro-patterned surfaces with a resolution of up to 300 nm [72].

The ability to self-clean has a considerably impact on the longevity of dry adhesives [65]. Results demonstrated that fabricating tiny fibrils from materials with high modulus of elasticity and low surface energy can improve the self-cleaning property of artificial dry adhesive surfaces [73–76]. The three types of self-cleaning are wet self-cleaning, contact-separation, and dynamic self-cleaning. Wet self-cleaning uses liquid to roll across the super-hydrophobic surface to remove dirty particles [63,77,78], contact-separation utilizes contacting with the attached surface to remove dirty particles [73,75], dynamic self-cleaning uses the mechanism of the gecko toes' hyperextension movement [40]. The self-cleaning function of the adhesive pads is used in climbing robots and grippers, but it has not been mentioned in the reports. Furthermore, most structures of artificial fibrils that can attach well to smooth surfaces show poor performance on rough surfaces. These adhesives cannot match the attachment ability of biological adhesive pads on rough surfaces [45,79].

2.2.2 Multilegged climbing robots

Many gecko-like feet with particular movement mechanisms and dry adhesives have recently been developed and successfully used in climbing robots as shown in Fig. 4 [24,55,57,80,81]. Unver et al. [82] developed a climbing robot called Geckobot with a tendon detaching mechanism on its feet. During the disengagement phase, cables driven by a servo arm pull up PDMS adhesives, and then compression springs can actuate the entire device back to its initial position. Stickybot, a gecko-inspired climbing robot developed by Stanford University, could climb through smooth vertical substrates, such as glasses, plastics, and tiles. The robot employs techniques inspired by geckos, such as hierarchical structure compliance, directional adhesion, and shear contact force adjustment, to achieve controllable adhesion [17,24]. A two-stage differential mechanism is employed to drive the toes for attachment and detachment with load-sharing, as shown in Fig. 4(a) [24]. Its feet are covered in nanoscale with arrays of microscopic, sloping polymer fibrils, this asymmetric adhesive structure is similar to geckos' setae for easy attachment and disengagement. Its force control method enables adhesion force control while promoting smooth adhesion and peeling between the adhesive pad and the substrate. Ulsan National Institute of Science and Technology developed the UNIclimb, a small climbing quadruped robot made with 3D printing. Its multilayer adhesive feet allow it to walk on varying angled walls and ceilings. The leg module of the robot uses the Hoekens linkage mechanism, which is powered by a single motor [83]. LEMUR 3, a large quadruped climbing robot developed by Jet Propulsion Laboratory (JPL), as shown
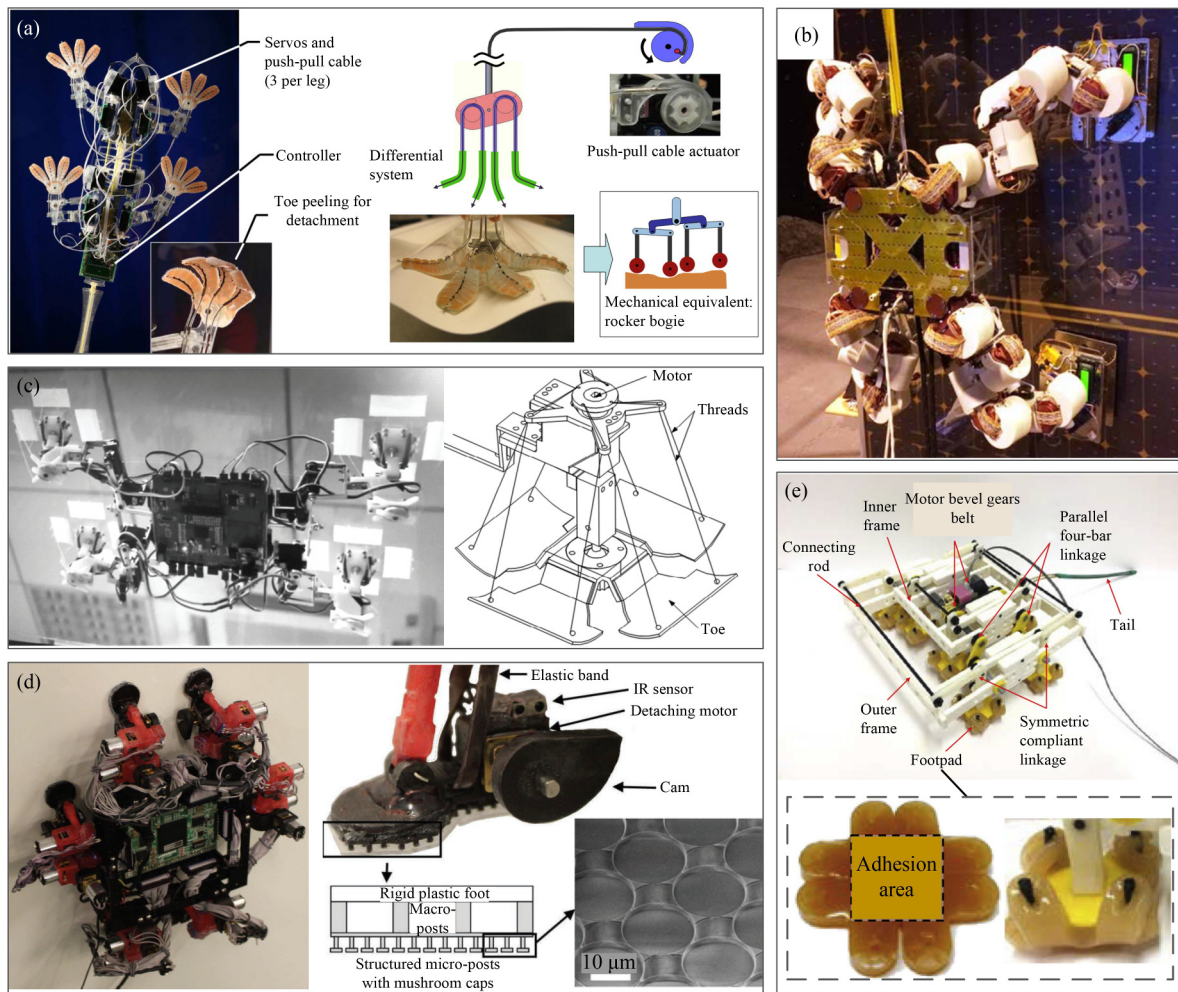
Fig. 4 Multilegged climbing robots with dry adhesives: (a) Stickybot and its foot, reproduced with permission from Ref. [24] from IEEE, (b) LEMUR 3, reproduced with permission from Ref. [57] from The American Association for the Advancement of Science, (c) gecko robot_7 and its foot, reproduced with permission from Ref. [55] from ACTA Press, (d) Abigaille-III and its foot, reproduced with permission from Ref. [80] from Springer Nature, and (e) AnyClimb II and its flat adhesive foot, reproduced with permission from Ref. [81] from Elsevier.

in Fig. 4(b) [57], can climb mock-solar panel surfaces using grippers covered with 80 μm anisotropic fibrils [19]. The adhesives are sheared by an opposite clamp mechanism for detachment and attachment, and the cable driving system can enable the load sharing between different adhesive pads [19,57]. Nanjing University of Aeronautics and Astronautics developed gecko robot_7, as shown in Fig. 4(c) [55], its feet can evert and stretch, similar to geckos' feet. Four PVS MSAMS adhesive surfaces are used as toes, which are connected with tendon-like threads driven by a motor. Furthermore, the surface of this toe is composed of two arcs, which can generate more normal adhesion than one arc and none arc structures [55]. Shao et al. [84] devised a hybrid soft-rigid foot with a sandwich structure, which was applied in the gecko-inspired climbing robot. The rigid component is used to provide sufficient pressure to achieve an omni-directional adhesive force. The soft part and dry adhesive with MSAMS are made by PDMS.

Increasing the number of legs on a legged climbing robot can enhance its gait stability. Birkmeyer et al. [85] devised CLASH, a micro six-legged wall-climbing robot with dual parallel four-bar legs to ensure foot posture. The ankle joint is a remote center-of-motion (RCM) mechanism constructed by a polyethylene terephthalate loop, a latex tendon, and an adhesive pad that allows the foot to make coplanar contact with the surface. Simon Fraser University's Abigaille II is a lightweight hexapod climbing robot [86]. Its feet are covered by arrays of flexible millimeter scale columns connected with a layer of MSAMS adhesive on the bottom. It can walk on vertical planes using a pentapedal gait. Its successor, Abigaille-III, employs dual-layer dry adhesives for attaching as well [80]. The detachment mechanism shown in Fig. 4(d) [80] is made up of an infrared ray (IR) sensor that detects contact and a cam that is powered by a detachment motor that peels off the adhesive pad. With the help of an elastic band, the foot can always be parallel

to the attached surface [80]. Yeungnam University developed the AnyClimb family of eight-legged wall climbing robots, as shown in Fig. 4(e) [81]. Vytaflex-10 elastomer is used to make the flat dry adhesives. A compliant asymmetric four-bar mechanism is designed to generate the motion trajectory of the foot when climbing on curved surfaces [81,87].

2.2.3 Wheeled and tracked climbing robots

On smooth and planar surfaces, mobile robots with wheels and tracks outperform legged systems in efficiency. Climbing robots that use wheels or tracks as climbing mechanisms have better speed and simpler structure, but they are less capable of overcoming obstacles than legged robots. Wheels and tracks can also have incorporated dry adhesives as shown in Fig. 5 [53,54,88,89]. Some climbing wheels are designed with dry adhesive feet around their rims to increase contact area. These wheels are known as whegs. Carnegie Mellon University's Waalbot II shown in Fig. 5(a) [88] is a small nimble wall-climbing robot; it is developed for climbing smooth vertical surfaces and is the first robot to use whegs for climbing. It was outfitted with Vytaflex-10 adhesives for climbing. Each wheg is triangular in shape with three adhesive pads and is powered by a gear motor. Each triangle vertex is attached by a passive revolute ankle joint to one foot with an adhesive pad. When the whegs revolve, the forward adhesive pad contact with the surface, and the rear adhesive pad separates from the surface to allow the robot to climb. It can also complete the transition from floor walking to wall climbing [88]. A passive revolute joint between the two sides of the robot is used in the updated version, Waalbot II [90]. It can enable each side to independently rotate to reduce internal tension between the feet on the opposite sides. The climbing robot Orion exploits bilayer dry adhesives to climbing at most 120° slope. Its dynamic model is built by an equivalent virtual model as a slider-crank mechanism [91]. Mini-Whegs, little climbing robots shown in Fig. 5(b) [54], climb using two whegs, each of

which has four MSAMS adhesive pads made of PVS. They can climb an inverted glass surface. The curvature profile of the foot helps keep the adhesive pad from curling back [54].

Adhesive tracks are easier to design than adhesive feet or whegs and modularized to satisfy the requirements of the user [53]. Carnegie Mellon University developed Tankbot, a tracked climbing robot family with six variants [89,92]. Tankbot family robots are lightweight, ranging from 60 to 150 g and can climb an incline with any angle ranging from 0° to 360° on smooth surfaces. They can stick to smooth substrates continuously and firmly, achieving relatively rapid and stable movements, obstacle negotiation capability, and load capacity. Vytaflex-10 is used as the material of the flat adhesive tracks. Its active tail can transfer the normal component of the peeling force to the front wheel to enhance the downward thrust on the front track, which regulates the track contact area with the connected substrate. Carnegie Mellon University developed MultiTank, a climbing robot, based on Tankbot's research by connecting two track modules via passive waist joints. Figure 5(c) [89] shows the prototype's structure, with A and B representing the two adhesive track modules, C representing the passive waist joint, D representing the active tail, and E representing the control board. TBCP-II employs two tank modules, as shown in Fig. 5(d) [53], with MSAMS adhesive tracks. Each module is actuated by a motor for adhesion and movement. These modules are linked by an active joint enabling active adhesive preloading based on feedback from distance measurements between the robot and the surface [53]. The waist joint can take the place of the tail in providing preload and enables it to complete the transition of movement from horizontal to vertical surface climbing.

2.2.4 Gripper

Dry adhesives are suitable for soft robotic grippers because of their similar material properties. Many soft grippers with dry adhesives are developed as shown in
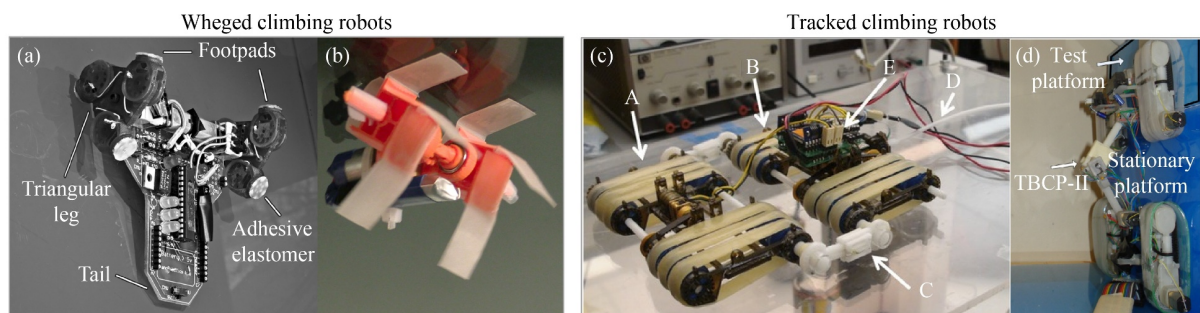

Fig. 5 Climbing robots with dry-adhesive wheels or tracks: (a) Waalbot II, reproduced with permission from Ref. [88] from IEEE, (b) Mini-Whegs, reproduced with permission from Ref. [54] from IEEE, (c) MultiTank, reproduced with permission from Ref. [89] from John Wiley and Sons, and (d) TBCP-II, reproduced with permission from Ref. [53] from IOP Publishing.

Fig. 6 [57,58,93–96]. Adhesive soft grippers can satisfy the requirements of a compliant interface for conforming to uneven surfaces as well as a strong grasp [93]. Dadkhah et al. [97] modified a Schunk gripper by grouping three electrostatic and dry adhesive pads to attach and grasp. Tendons are used to load in a shear for flat surfaces. The tests show that the gripper works well on various smooth and rough surfaces including textiles. Song et al. [93] devised a soft-gripping device for grabbing nonplanar 3D geometries that incorporate an elastomeric adhesive and a pressure-controlled deformable gripper body, as shown in Fig. 6(a). It controls adhesion strength by adjusting internal pressure and using the mechanical principle of load sharing at the interface.

On irregular surfaces, the soft adhesion system can employ up to approximately 26% of the maximum adhesive, it is 14 times greater than the stiff adhesion system without load-sharing [93]. Stanford University developed a robotic gripper for grasp in microgravity that consists of a flat surface gripper unit covered with wedge-shaped fibrils [98], a curved surface gripper unit also covered with adesives, a pulley differential load-sharing system, and a nonlinear passive wrist with four super-elastic shape memory alloy (SMA) for increasing compliance, as shown in Fig. 6(b) [57]. It can grasp objects with diameters from 0.6 to 2.2 m, and its maximum payload reaches 400 kg [57]. JPL developed a gripper by combining fluidic elastomer actuators and an
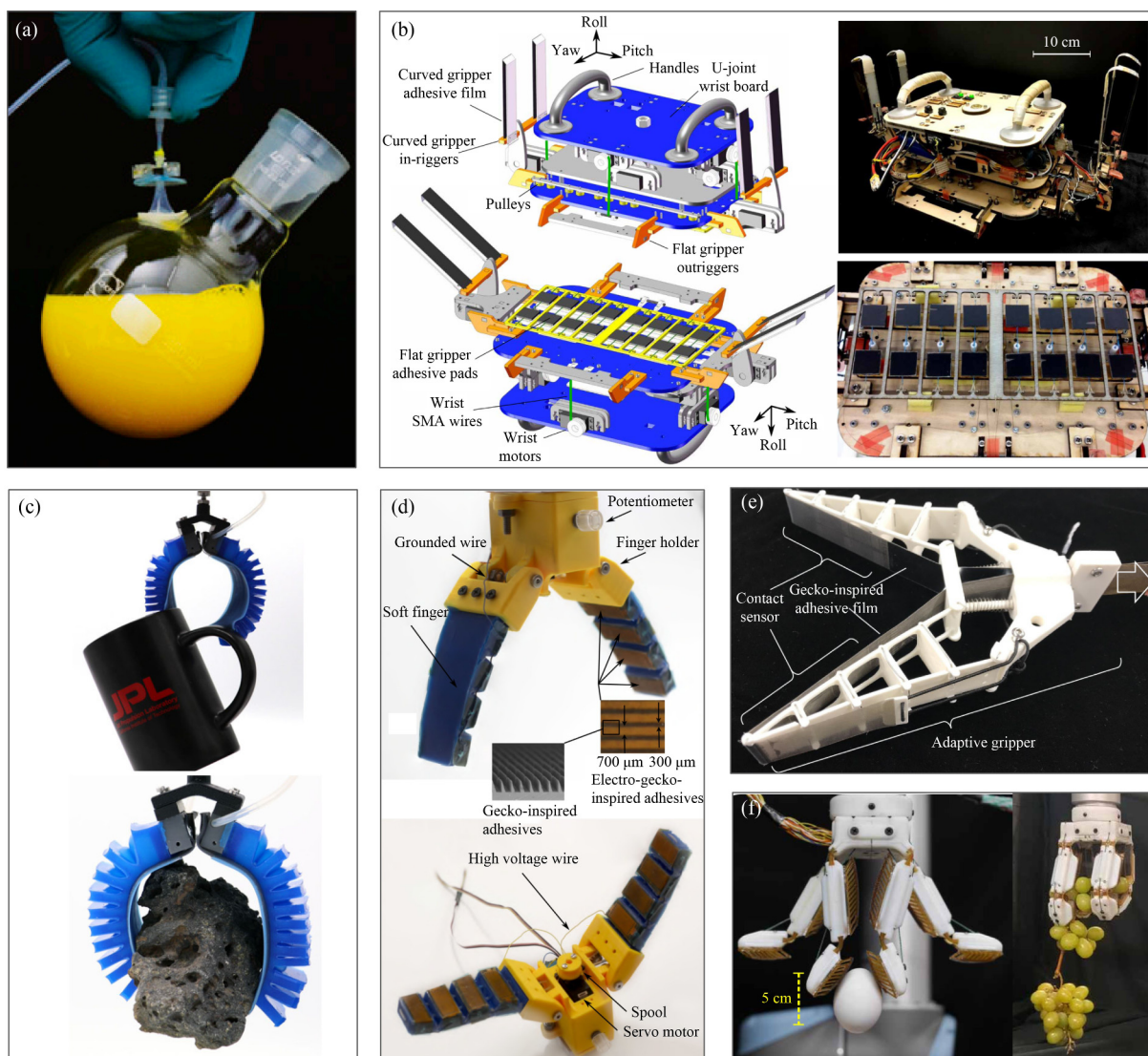

Fig. 6 Robotic grippers with dry adhesives: (a) sucker covered with dry adhesive [93], copyright 2017, (b) gripper for manipulation in microgravity, reproduced with permission from Ref. [57] from The American Association for the Advancement of Science, (c) gecko-adhesive elastomer actuator grippers, reproduced with permission from Ref. [94] from IEEE, (d) soft gripper with dry adhesives and electrostatic adhesives, reproduced with permission from Ref. [58], (e) adaptive soft exoskeleton gripper with the directional adhesive, reproduced with permission from Ref. [95] from IEEE, and (f) farmHand, reproduced with permission from Ref. [96] from The American Association for the Advancement of Science.

artificial dry adhesive. On dusty or rough surfaces, where dry adhesion is ineffective, the soft gripper can preserve grasp ability through fluidic elastomer actuators, as shown in Fig. 6(c) [94]. Hao et al. [99] developed a cylindrical accordion-shaped soft gripper with an interior gecko-like adhesive surface to increase attachment force. An object would be enveloped or grasped when it is inflated or deflated by pressure produced by fluidic channels. The gripper adapts better to the shape of the object than grippers with soft fingers. Illinois Institute of Technology developed a soft gripper with two fingers covered by dry adhesives and electrostatic adhesives for grasping objects with a wide range of roughness as shown in Fig. 6(d) [58]. The geometry for the electrodes is optimized by Comsol Multiphysics software to improve the grasp wrench of the gripper. Hu et al. [100] devised a bioinspired soft gripper with two branches that consist of flat dry adhesives, soft actuators by SMA, and microspines. The integrated gripper can lift regularly or irregularly shaped objects with smooth or rough surfaces, thereby providing a higher adhesive force than the non-adhesive type. Hashizume et al. [95] developed an adaptive underactuated gripper combined with a capacitive sensor and a dry adhesive film, as shown in Fig. 6(e). Each finger skeleton is made up of a bendable inner soft beam that conforms to curved surfaces and a flexible chain of segments connected by pins to cross beam struts. The fingers are 3D printed by ABS plastic. When employing adhesive films, the gripper may reach 2.6 times the pull out force on rough surfaces when compared with soft rubber [95]. Stanford University developed a tendon driving anthropomorphic robotic gripper called farmHand with four fingers composed of the rigid phalanges and the flexible buckling ribs as adhesive suspension [96]. Its adhesive suspensions can improve the contact area and the load sharing in tangential and normal direction. It can grasp objects of various sizes and hardnesses (such as grapes, eggs, apples, and 3 kg orange juice buckets), as shown in Fig. 6(f) [96].

3 Wet adhesion

Many living organisms, such as tree frogs and insects, can perform secretions from adhesive pads to build liquid bridges between contact units (e.g., nanopillar and seta) and attached substrates, generating viscosity and capillarity force or constructing fixation, which is commonly referred to as wet adhesion [11,101]. The adhesive methods of tree frogs, walking stick, mussels, and some other organisms have inspired the development of bionic adhesives used in robots.

3.1 Mechanisms of wet adhesive

Tree frogs can climb easily and freely on rough surfaces,

such as barks, by injecting a mucus into the pad-substrate contact area to generate wet adhesion [102]. Convex epithelial cells are mainly hexagonal with nanopillar tips on extremely soft toe pads of tree frogs to adapt and match well with irregular surfaces [103], as shown in Fig. 7 [11]. Wet adhesion can inspire us to design practical wet adhesive surfaces and corresponding attachment devices to use in robotics and medicine.

When a filmy layer of liquid covers the pace between the contact units on the biological attachment pad and the attached substrate, the wet adhesion is usually ascribed to capillary forces and Stefan adhesion demonstrated by a model shown in Fig. 8. It is constituted by a contact unit on a plane substrate and connected by a drop of liquid. When the detachment occurs, the corresponding force against capillarity force F_{cap} is given by Eq. (2), as follows:

$$F_{cap} = -\pi R^2 \gamma \frac{\cos\theta_1 + \cos\theta_2}{h} - \pi R \gamma, \qquad (2)$$

where R is the radius of the contact unit, γ is the surface tension, h represents the height of the liquid film, and θ_1 and θ_2 are the contact angles of the liquid film with contact unit and the surface, respectively. When separation occurs in two surfaces involving the fluid in the gap between them, a viscous force will resist the separation until the movement is completed. The hydrodynamic force F_{hyd} can be given, as follows:

$$F_{hyd} = -\frac{dh}{dt}\frac{3\pi\eta R^4}{2h^3}, \qquad (3)$$

where η is the viscosity of the liquid, and t is the separating time of the two surfaces [104–106]. The capillarity forces are mainly decided by the radius of the contact unit, and viscous forces are dominated by separation speed. Capillarity forces and Stefan adhesion would decrease when the liquid layer height h increases. In a recent study [107], the model with multiple liquid drops is established for enhancing capillarity forces, in which one large liquid droplet with volume of V is regarded as n small drops with volume of V/n. The corresponding capillarity force equation of multiple wet adhesion $F_n(d)$ is described as follows:

$$F_n(d) = 2\pi n^{2/3} \gamma s f(dn^{1/3}), \qquad (4)$$

where n represents the number of contact units, s is the scale factor, d is the normalized separation, and f is the normalized total force. Equation (4) demonstrates that the capillarity increases significantly when the number of liquid drops increases.

For example, the wet adhesion studies on tree frogs are mainly generalized from the unique morphology of their toe pads and features of mucus as a viscous agent secreted by their toe pads. Barnes [11] proposed that the non-Newtonian fluid models of a little liquid drop of mucus play an important role in regulating adhesion
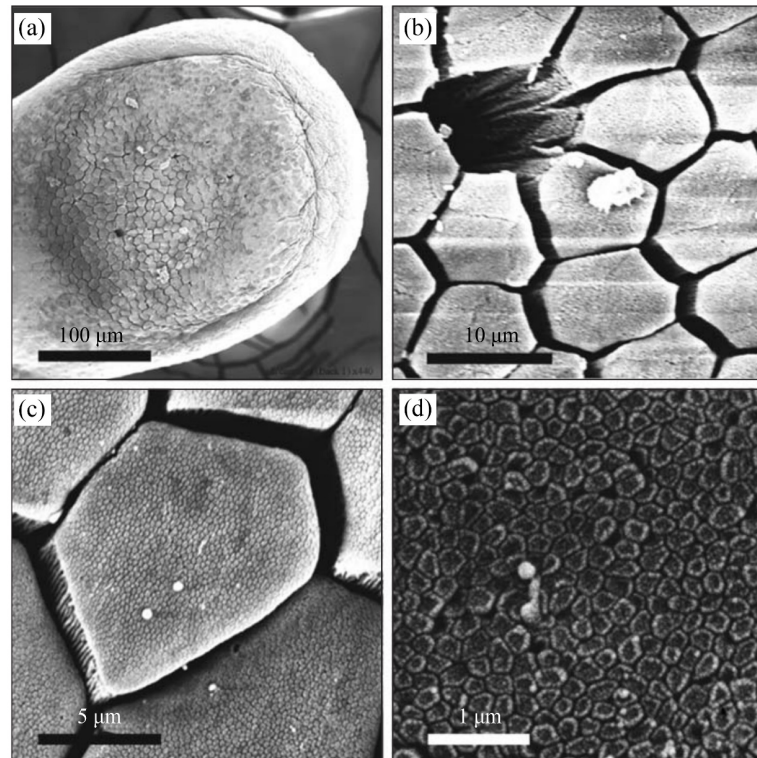
Fig. 7 Tree frog toe from macro to micro, reproduced with permission from Refs. [11] from Springer Nature: (a) whole toe pad, (b) toe pad epidermis showing largely hexagonal columnar epithelial cells, the channels between them and a mucus pore, (c) view of a single epithelial cell showing evidence of nanostructuring on its surface, and (d) view of part of the surface of a single epithelial cell showing nanoscale peg-like projections.
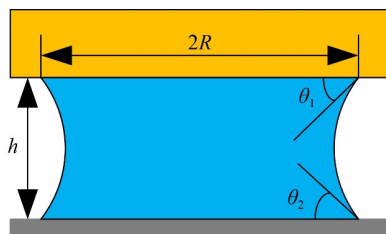

Fig. 8 Wet adhesion model.

force. Then, Persson [102] established the model of the adhering and peeling process between adhesive pads and attached surfaces on the basis of the capillary forces. The reversible adhesion can be achieved by regulating the distance between the attached surfaces and the toe pad by using the channels on the glands of pad, which can absorb and release the liquid. These channels can also apply mucus to the pad surface and remove water on the attached surfaces to achieve wet adhesion [103]. Moreover, the self-cleaning property of the adhesive toe pads after contamination was studied, and the results showed that shear motion and the washing effect of the secreted mucus could assist in shedding dirty particles on the contact surface [108]. Tulchinsky and Gat [109] proposed that the viscous-poroelastic interaction was a temporary adhesion mechanism of tree frogs. The

physical and mathematical models are set up, showing that stress at the contact area could cause transitory adhesion. Therefore, the mucus secreted by adhesive pad of tree frogs can assist in generating wet adhesion on the attached surfaces by its multiple functions, such as flushing and viscous agents, generation of capillary force, viscous force and the viscous-poroelastic interaction, and self-cleaning property.

Generally, the unique functions and morphology of the adhesive pads of tree frogs and their special mucus play a decisive role for the formation of wet adhesion. Thus far, the wet adhesion mechanism of tree frogs has not been fully revealed. More studies should be carried out to clarify the essence and mechanisms of wet adhesion, such as mucus control method and effect of different mucus compositions [110].

In addition to organisms that use adhesive pads for attachment in wet conditions, mussels and sandworms have been discovered to use hydrogels to generate adhesion [111]. The ability to adhere is dependent on the production of sticky protein glues. 3,4-dihydroxy-l-phenylalanine, a catecholic amino acid included in sticky protein glue, has been demonstrated to permeate the hydration layer and interact with the substrate surface [112]. According to recent reports, researchers can design reversible attachment of hydrogels for use in climbing robots [113].

3.2 Wet adhesives

Various artificial wet adhesives have been developed in recent years by mimicking the hexagonal structures of tree frog toe pads as shown in Fig. 9 [114–116], and their wet adhesive properties have been extensively studied. Many materials with a wide range of Young's module, such as carbon nanotube, polyurethane (PU), polyurethane acrylate (PUA), polystyrene (PS), and PDMS, are used to fabricate wet adhesives using various manufacturing methods [110]. The aspect ratio (AR) of micro column is very critical given its stability and adhesive performance [117]. Generally, increasing AR increases wet adhesion significantly [114], but higher AR does not always contribute to enhanced adhesion. The probability of bending and clustering of micropillars is increasing when the space between micropillars is extremely small [118,119]. Chen et al. [114] studied wet adhesives employing various micropillar patterns including quadrangle, triangle, rhombus, and diverse hexagon, they found that the surfaces with hexagonal pillar shown in Fig. 9(a) can provide stronger friction. The surgical grasper with hexagonal micropillar performs better on friction and deformation than conventional surgical grasper [114]. The wet adhesives having complex microstructure of PS fibrils combined with soft PDMS hexagonal pillars can significantly increase adhesion and friction compared with the microstructure with only PDMS. This structure can also adjust the stress distribution of interface during contact, such that wet adhesion can be enhanced by reducing the maximum stress and moving the maximum stress to the central area [120].

The study shows that adding a thinner PDMS layer at the end of the PS column can more effectively reduce the stress on the edge of the column and enhance adhesion [120]. Similarly, T-shaped PUA micropillars covered with a film of PDMS can bear larger shear force than T-shaped micropillars only made of PDMS or PUA. The wettability of microstructure surface also has a profound influence on wet adhesion [121]. Drotlef et al. [121] studied the attachment mechanism of wet adhesives made of PDMS with diverse wettability. They proposed that when a liquid film is present, capillary force and contact force determine the wet adhesion of a surface with micropattern together. Furthermore, few studies demonstrate that adhesives with narrow hexagonal or unique arch-shaped microstructures shown in Fig. 9(b) [115] could generate more friction under humid conditions than standard hexagonal micropatterns, possibly due to superior drainage performance [115,118]. Although most studies on wet adhesion employ covering a liquid film over adhesives, some studies transport the mucus to the contact zone to imitate biological secretions, as shown in Fig. 9(c) [116].

3.3 Applications in robotics

Wet adhesion is less common in robotics than dry adhesion, but it has been growing in popularity in recent years. These robots are primarily used on wet surfaces and lack the ability to secrete mucus autonomously. The application of wet adhesives in reversible adhesion is limited because the key technology of automatic liquid secretion and micro-control methods has not yet broken through. Figure 10 [104,122–124] displays a few typical instances of wet adhesion applications in robotics. Suzuki et al. [125] designed a wall climbing robot inspired from ants; it uses a wet adhesive glass pad to generate normal force and dry adhesive PDMS pads to generate tangential forces. Tongji University developed a walking stick-inspired wet adhesion pad with quadrangle microstructure prepared using a combination of electroforming and soft lithography [126]. It was used in a hexapod climbing robot, which can climb on the 80° smooth surface, as shown in Fig. 10(a) [104]. Chen et al. [122] used wet adhesives on the center of a microrobot Harvard Ambulatory MicroRobot (HAMR) to generate adhesion by capillary force, as shown in Fig. 10(b). The microrobot slides using four legs to accomplish its climbing movement. Xiamen University researchers developed a borate ester polymer hydrogel that can rapidly switch between adhesion and non-adhesion in response to mild
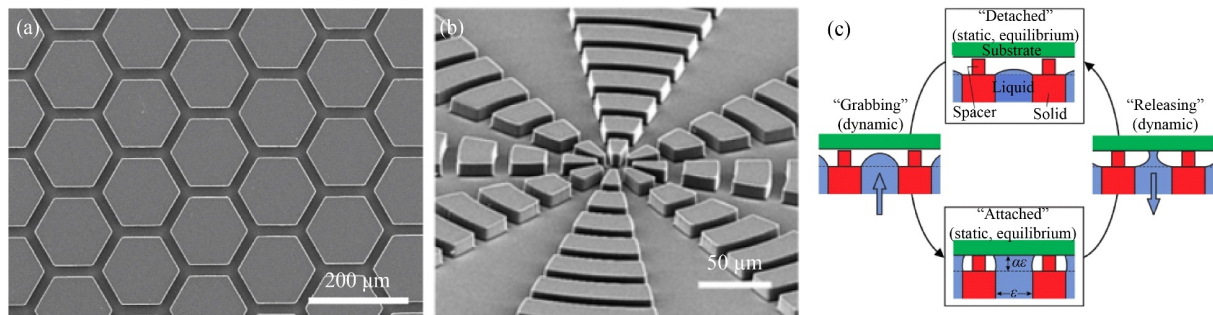

Fig. 9 Wet adhesives: (a) wet adhesives with hexagonal pillars, (b) wet adhesives with arc pillars, and (c) reversible adhesion by pumping liquids in and out. Reproduced with permission from Refs. [114–116] from American Chemical Society.
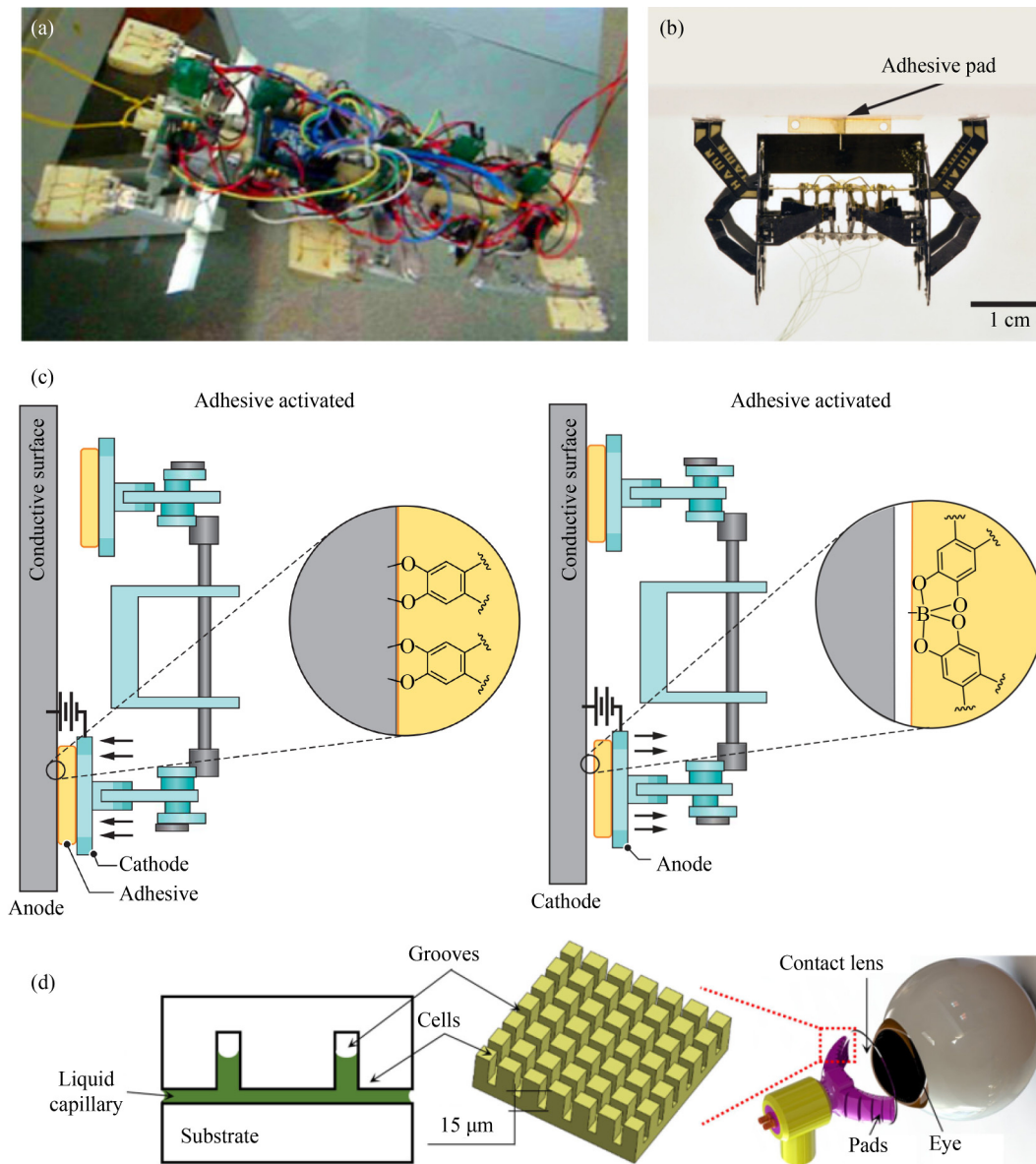
Fig. 10   Applications of wet adhesion in robotics: (a) hexapod climbing robot, reproduced with permission from Ref. [104] from IEEE, (b) insect-scale climbing robot with wet adhesives, reproduced with permission from Refs. [122] from IEEE, (c) illustration of the robot climbing by hydrogel, reproduced with permission from Refs. [123] from The American Association for the Advancement of Science, and (d) soft gripper with wet adhesives, reproduced with permission from Refs. [124] from IEEE.

electrical stimulation [113]. The hydrogel can repeatedly adsorb and separate different surfaces by changing the direction of the electric field, with response times as short as 1 s. This hydrogel can be simply applied to the foot and wheel of climbing robots to enable them to climb on vertical and inverted conductive substrates (e.g., stainless steel and copper), as shown in Fig. 10(c) [123]. Xin et al. [127] developed a soft robot inspired by a snail and driven by pneumatic actuator, they increased the robot's crawling speed by 2.7 times by covering the contact surface with bionic mucus. Such climbing robots have potential applications in wet and slippery environments, such as the human body.

Nguyen and Ho [124] investigated the grasping of deformable thin shells using a soft gripper with microstructured wet adhesives. They developed a platform for automatic attachment and removal of contact lenses from the human eye in a humid environment, as shown in Fig. 10(d) [124]. The grasp forces were modeled and validated, and the results showed that grippers with square microstructured wet adhesion pads required 1.1–2 times less preload than those without microstructures. Van Nguyen et al. [128] also used similar wet adhesives in another pneumatic soft gripper with two fingers, which can grasp tofu with lower preload than common soft gripper.

4 Mechanical adhesion

Mechanical adhesion is defined in this context as the use of biological organs to hook, catch, interlock, or clamp onto asperities or structures on a surface to generate attachment forces, as shown in Fig. 11 [6,11]. Many animals, including birds [105,129], lizards [6,130], cats, and insects [6,105], cling well by interlocking claws or spines with substrates. Claws and spines can withstand enormous forces per unit area by catching protrusions and clinging to rough, hard surfaces [131]. They can also penetrate soft surfaces and cause adhesion [132]. Attachment failure is primarily caused by the rupture, bending, or yielding of the attachment devices or the attached surfaces [131]. In comparison to dry and wet adhesion, mechanical adhesion is a relatively macroscopic adhesion. The most common method of bioinspired mechanical adhesion in robotics is using claws to assist robots to attach on rough surfaces.

4.1 Biological devices

Insects and arthropods may readily climb on rough surfaces, typically using clawed legs and a plethora of small, sharp spines, s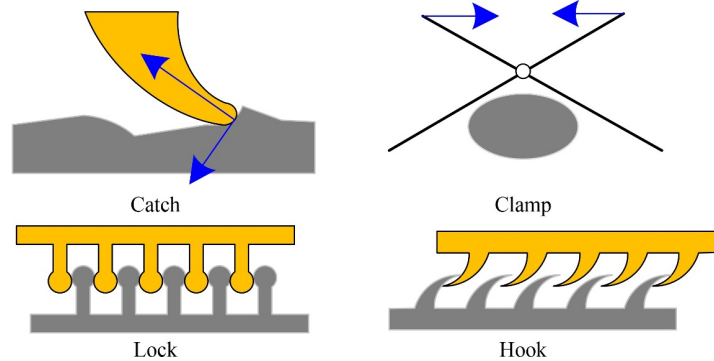uch as the cricket leg shown in Fig. 12(a) [133] that can interlock asperities. Frantsevich and Gorb [134] investigated the attachment of the hornet and built an equivalent mechanism of its tarsal chain, which has only one active degree of freedom (DOF), as shown in Fig. 12(b). The hornet can use two claws on the tarsus to grasp asperities on rough surfaces and a wet adhesive pad to cling to smooth surfaces [134]. When asperities on the surface are clasped by the claws of two opposing legs, the hornet can withstand external forces roughly 25 times its own weight [134]. Locusts (*Schisto-cerca gregaria*) are well-known for their powerful flying, jumping, and gripping abilities. Locusts can climb in surfaces with a wide variety of roughness using their sophisticated multi-functional tarsal chain containing adhesive pads, spines, and claws [135]. Han et al. [136] discovered that locusts (*Locusta migratoria manilensis*) can firmly cling to the ceiling when the diameters of asperities on the substrate are substantially larger than the diameters of the claw tips. The locust uses microspines to maximize the possibility of interlocking and matching mechanical adhesion for sustaining the main force, and the adhesive pads are employed passively to saturate the adhesion to avoid slippage during jumping [136]. Roderick et al. [129] observed the landing process of pacific parrots. They found that they mix predictable toe pad friction with probabilistic friction from their claws,

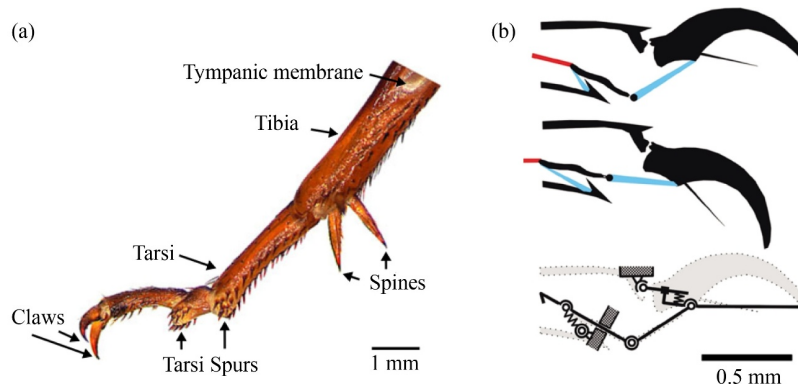**Fig. 11** Illustration of typical mechanical adhesion.

Fig. 12 Spines and claws of insects: (a) claws and spines on the cricket leg [133], copyright 2018, and (b) equivalent mechanism of the hornet claw, reproduced with permission from Ref. [134] from Elsevier.

which they drag to search surface protrusions. The claws should be dragged further when the toe pad is squeezed less. The findings were used to the design of an unmanned aerial vehicle landing mechanism [137].

Larger animals are more likely to slip or fail in intersection when using mechanical adhesion because of their greater weight, even if this effect depends on the scale of claw sharpness. Moreover, larger animals cannot avoid stress concentrations. This size-related decline in clinging performance has a substantial impact on larger animals' attachment capability [138].

The interactions between spines or claws and associated substrates are generally studied on 2D cross sections [139]. Dai et al. [4] investigated the anti-sliding forces between abrasive paper asperities and the claw tip of *Pachnoda marginata* (*Coleoptera, Scarabaeoidea*), a type of beetle without an adhesive pad. A planar model demonstrating the saturated friction that could be increased with increasing surface roughness was proposed. When the roughness of the substrate is substantially more than the dimension of the claw end, as shown in Fig. 13(a) [4], the beetles can use their claws to catch with surface structures, resulting in a stable mechanical interlock. From the equilibrium condition, the limiting scenario may be deduced, as follows:

$$\frac{F}{W} = \frac{\cos\alpha + \mu\sin\alpha}{\sin\alpha - \mu\cos\alpha} = \frac{1 + \mu\tan\alpha}{\tan\alpha - \mu}, \quad (5)$$

where F is the shear force along the attached substrate, μ represents friction coefficient between claw end and attached surface, and W is the weight acting on the claw directed normal of the attached surface. α represents the contact angle, which can be defined as

$$\sin\alpha = \frac{r_{tip} + h_{asp}}{r_{tip} + R_{asp}}, \quad (6)$$

where r_{tip} denotes the radius of the claw tip, R_{asp} denotes the radius of the asperity, and h_{asp} denotes the depth of the center of the asperity, as shown in Fig. 13(a) [4].

Asbeck et al. [139] built a clinging model of a single spine, as illustrated in Fig. 13(b), and successfully implemented a wall climbing robot in Spinybot II. The microspine is represented as a circle with radius r_s approaching the attachment surface in a direction close to the vector; it slides outside the attached surface and sweeps out a volume. The center of the tip can be tracked to produce a traced surface. The microspine can perch where the angle between the approach vector and the vertical direction is greater than the critical attachment angle θ_{min}.

$$\theta_{min} = \theta_{load} + \text{arc}\cot\mu, \quad (7)$$

where θ_{load} is the angle between the surface and the direction of external force. These types of attachment model are widely used in bioinspired climbing robot working on rough surfaces.

4.2 Applications of mechanical adhesion in robotics

Climbing robots working on hard, rough outdoor surfaces rarely use adhesive pads due to limitations in self-cleaning ability and abrasion resistance, and mechanical adhesion is the optimal approach to adhere to such surfaces. Various rigid-flexible spine mechanisms inspired by biological claws and microspines have been effectively employed in climbing robots working on rough surfaces. In grasped surfaces with complex morphology, such as tree trunks and boulders, grippers with microspines can achieve force closure, resulting in stable attachment. Such attachment devices have a bright future in ocean exploration and asteroid detection. In addition, spines and claws can be used on the feet of jumping robots and bipedal robots to prevent slippage [135,140].

4.2.1 Bioinspired spine mechanisms

The spine or claw systems can be applied in the attachment to substrates that should be sufficiently rough to supply contact points for perching with low energy consumption. Even a power outage will not necessarily cause system failure if the mechanical adhesive settings
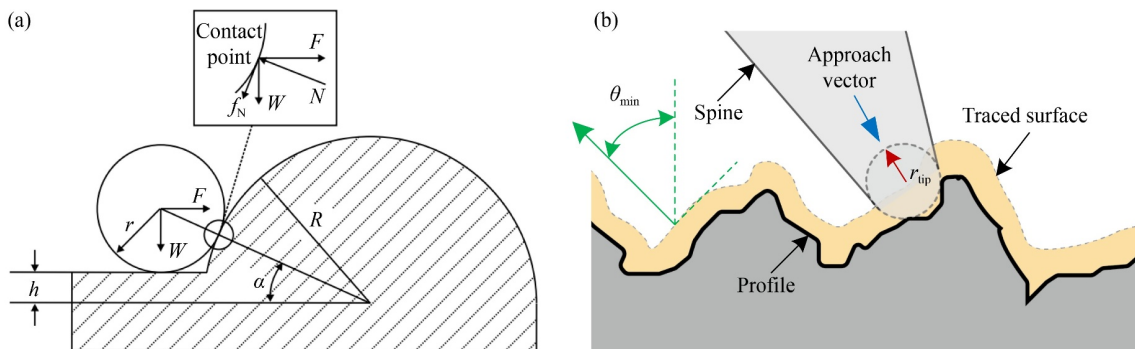

Fig. 13 Mechanical interlock models: (a) planar model of interlock between the beetle claw and the rough surface, reproduced with permission from Ref. [4] from Company of Biologists Ltd., and (b) planar model of interlock between the spine and the rough surface.

support it. However, such systems are slow and have limited operability, and their payloads are smaller than those of magnetic or pneumatic climbing robots.

Climbing robots that operate on centimeter-level roughness surfaces are often outfitted with bioinspired spine mechanisms on their feet, wheels, or grippers. The two broad types of bioinspired spine mechanisms are compliant long-flexure spine mechanisms and linearly-constrained spine mechanisms as shown in Fig. 14 [19,141]. Compliant long-flexure spine mechanisms can be developed through some types of additive manufacturing, which allows the combination of multiple materials, as shown in Fig. 14(a) [19], or through compliant mechanism with a single material, as shown in Fig. 14(b) [141]. Asbeck et al. [139] investigated the stiffness feature of this type of spine mechanism.

Developing a spine mechanism with the desired stiffness parameters can maintain load-sharing between spines, increase the possibility of catching asperities by stretching in tangential, and prevent the robot from pushing off from the wall by normal contact force. The linearly-constrained spine mechanism design shown in Fig. 14(c) has a higher density of stingers with independent suspension above each spine, allowing for better adaptation to uneven surfaces, such as rocks [142].

4.2.2 Applications in feet of legged climbing robot

To enable climbing movements, spine mechanisms can be used in the feet of hexapod robots, such as RiSE V2 in Fig. 15(a) [18], quadruped robots, such as claw inspired robot (CLIBO) in Fig. 15(b) [143], and biped robots, such
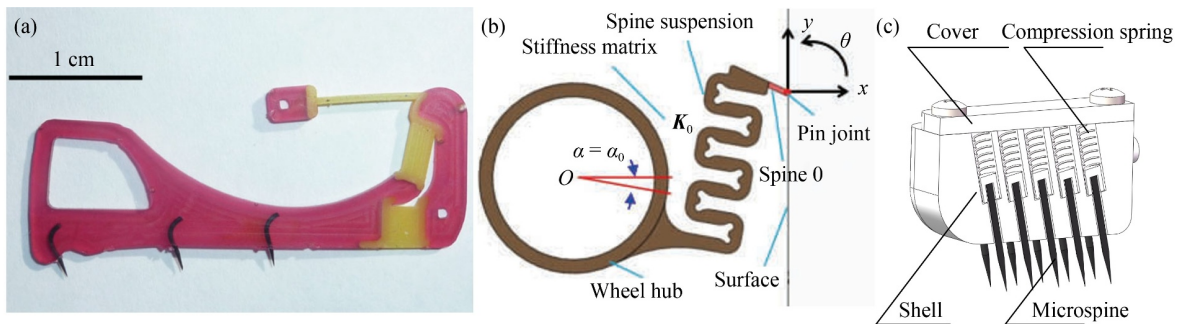
Fig. 14 Bioinspired spine mechanisms: (a) compliant long-flexure spine mechanism with two types of materials, reproduced with permission from Ref. [19] from John Wiley and Sons, (b) compliant long-flexure spine mechanism with a single material, reproduced with permission from Ref. [141] from Springer Nature, and (c) cross-section of a linearly-constrained spine mechanism.
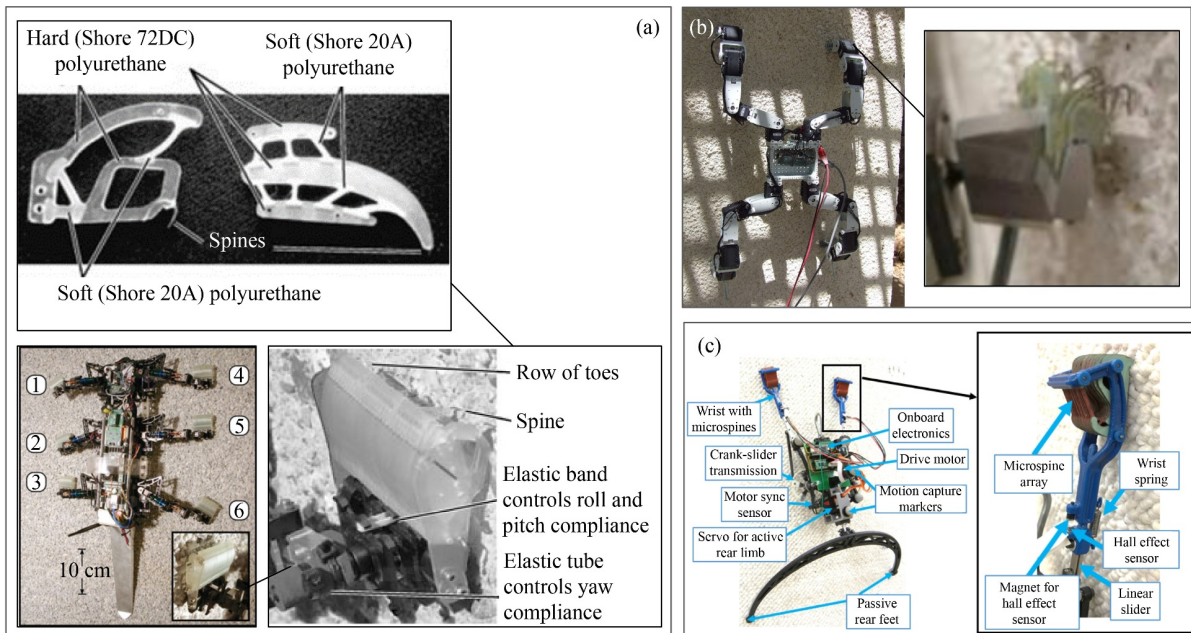
Fig. 15 Applications of bioinspired spine mechanism in legged robots: (a) RiSE V2, its foot and toes, reproduced with permission from Ref. [18] from John Wiley and Sons, (b) CLIBO, reproduced with permission from Ref. [143] from Elsevier, and (c) BOB 2.0, reproduced with permission from Ref. [144] from IOP Publishing.

as BOB 2.0 in Fig. 15(c) [144]. Spinybot II, developed by Stanford University, is the first legged climbing robot that can walk on outside construction surfaces (e.g., brick, cement, and stone) using microspines. Shape deposition manufacturing (SDM) [145] is used to fabricate the microspine mechanism, which permits hard and soft materials to be integrated as a single structure. Soft PU, which provides elasticity as well as viscoelastic damping, can allow greater extensions without failure compared with steel springs [139]. The toes of the hexapod climbing robot RiSE V2 are also made by SDM, as shown in Fig. 15(a) [18], they are typical compliant long-flexure spine mechanisms. Arrays of these toes are combined in a foot with hierarchical compliance. The foot is linked to the robot via a universal joint. CLIBO is a quadruped climbing robot, and its each foot is outfitted with 12 claws made of fishing hooks, allowing CLIBO to cling to and climb on rough walls [143]. Some biped climbing robots with spiny feet, such as BOB 2.0 [144] and DynoClimber [146], can perform dynamic climbing on rough walls. Their claw-like toes are similar to those of RiSE [146]. Hu et al. [147] devised an inchworm-inspired climbing robot that consists of soft body and spiny feet. The soft robot is actuated by SMA wires and utilizes microspine arrays to attach its feet to rough or soft surfaces.

4.2.3 Applications in wheeled and tracked climbing robots

Microspines can be arranged on the wheel or the track edge to enable climbing robots to complete attachment and locomotion as shown in Fig. 16 [141,148]. On flat surfaces, climbing robots with spiny wheels are typically faster and more efficient than legged climbing robots with spiny feet. Tbot, a wheeled wall climbing robot developed by University of Science and Technology of China, can climb hard rough surfaces, such as concrete and brick walls, using two compliant spiny wheels and a tail. Tbot can transit from horizontal to vertical planes effortlessly. As illustrated in Fig. 16(a) [141], the compliant spine mechanism is made up of a microscopic spine and an elastic suspension that connects the microspine to the wheel hub. The stiffness characteristic

of *Sericaorientalis Motschulsky* inspired the spine mechanism of Tbot. The elastic suspension is 3D printed from PA2200 nylon. The microspines are approximately 1 mm long, with shaft diameters of 200 mm and tip radiuses of 30–60 μm [141]. JPL developed the crash-proof robotic family, which includes seven different types of robot weighing from 80 to 540 g. Their wheels are made up of 10 to 40 separate rotary microspines to ensure that at least one or two hooks catch asperities and support the robot. The hub of these wheels is a combination of two hardnesses of PU using the SDM process to achieve rigid−flexible coupling. These robots can climb stairs and rough vertical walls [149]. SpinyCrawler, a track-type climbing robot, can generate adhesion by using a spiny track with an opposing grasping mechanism, as shown in Fig. 16(b) [148]. The body of the spine mechanism is 3D printed by nylon. For attachment and disengagement, a cam mechanism is included into the robot design without the need of additional actuators [148].

4.2.4 Applications in robotic grippers

Although arrays of microspines can efficiently hook asperities on rough surfaces, such as concrete walls and trees, to provide mechanical adhesion, they struggle to adapt to the complicated topography of surfaces, such as rock, where they rapidly lose stability. Furthermore, when the angle of incline is greater than 90°, generating sufficient normal adhesion can be difficult. Many spiny gripers, inspired by birds and lizards, have been designed to generate force closure and provide greater adhesion by combining grasping and hooking such as examples in Fig. 17 [19,132,150–152]. As shown in Fig. 17(a) [19], JPL developed a robotic gripper with spiny fingers; it is used in LEMUR, a family of rock-climbing robots designed to investigate severe terrain on Mars or asteroids. Its microspines resemble those of RiSE V2. Each gripper contains around 250 microspines that are uniformly distributed throughout 16 carriages. The carriages can move freely and conform to centimeter-level roughness due to elastic components. A linear motor for engagement and three other linear motors for disengagement linked to carriages by cables are available.
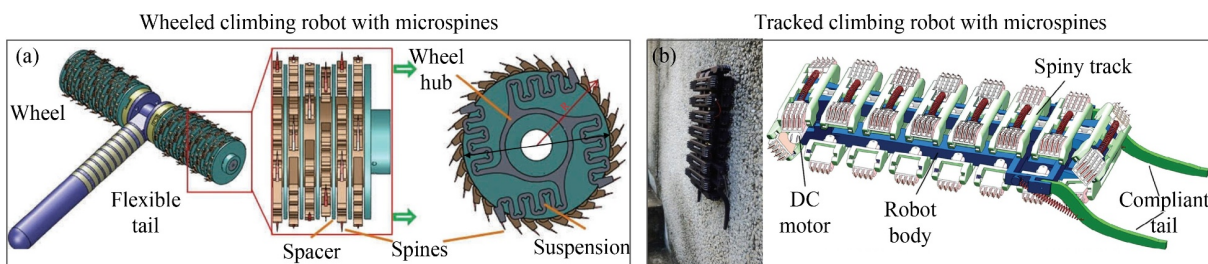

Fig. 16 Applications of bioinspired spine mechanism in wheeled and tracked climbing robots: (a) Tbot, reproduced with permission from Ref. [141] from Springer Nature, and (b) SpinyCrawler, reproduced with permission from Ref. [148] from Springer Nature.
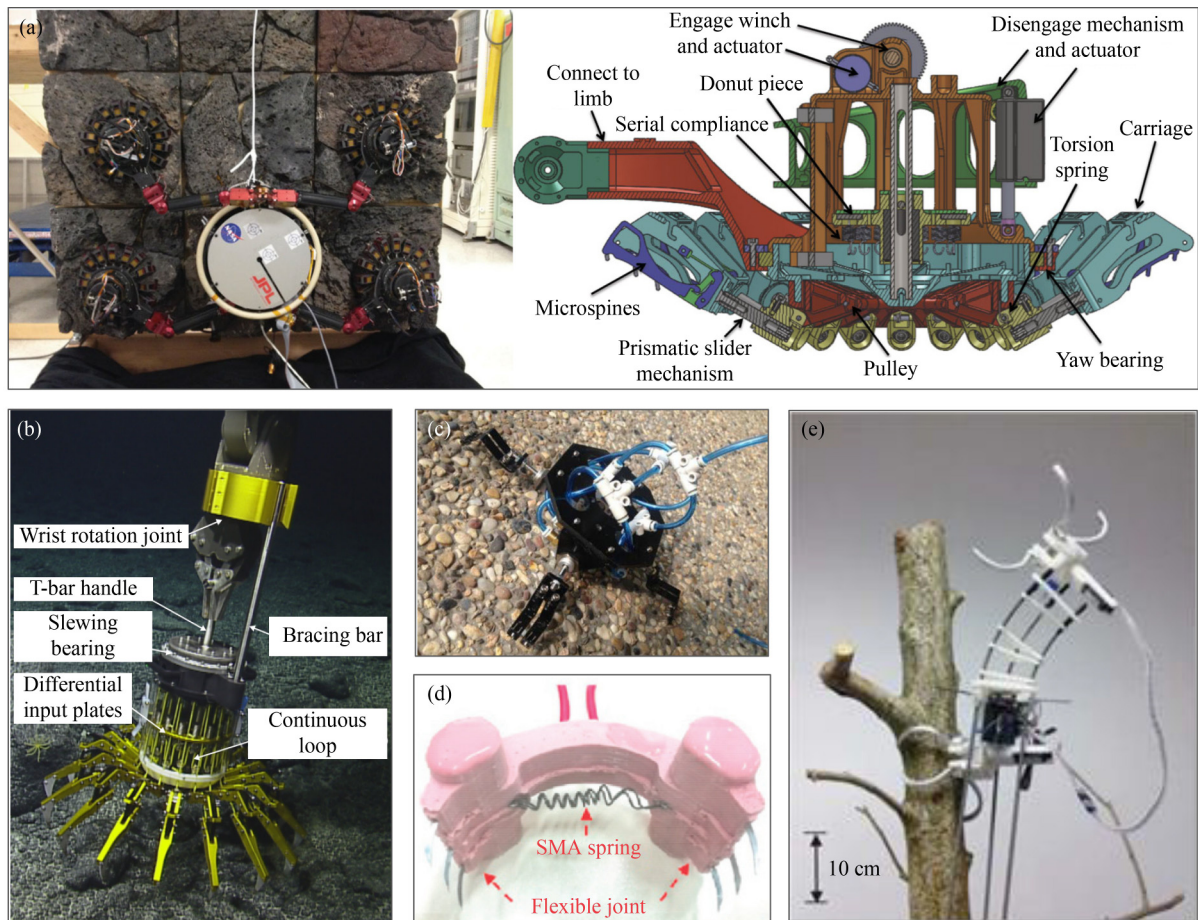
Fig. 17 Application of mechanical adhesion in robotic grippers: (a) LEMUR IIB and its gripper, reproduced with permission from Ref. [19] from John Wiley and Sons, (b) JPL-Nautilus gripper, reproduced with permission from Ref. [150] from John Wiley and Sons, (c) pneumatic gripper with claws, reproduced with permission from Ref. [151] from Springer Nature, (d) soft spiny gripper, reproduced with permission from Ref. [152] from IOP Publishing, and (e) Treebot, reproduced with permission from Ref. [132] from John Wiley and Sons.

On vesicular basalt, the gripper can withstand 281.4 N tangent force and 189.5 N normal force with a weight of 1.05 kg [19]. LEMUR 3 can scale cliff sides using its microspine grippers [25,153]. However, because the attachment and disengagement processes are extremely complex, the climbing speed of LEMUR 3 is very slow. Furthermore, reports showed a 5% possibility of disengagement failure [19]. In the future, this type of gripper can also be used for asteroid and ocean sampling [19,150]. As shown in Fig. 17(b) [150], the JPL-Nautilus gripper is an underactuated spiny gripper with 16 fingers made up of four bar linkage microspines and a tendon driving system. It can generate 450 N by anchoring rocks and grasp objects ranging in size from 10 to 30 cm underwater. Princeton University developed a spiny gripper for grasping rock faces in preparation for future asteroid exploration. The gripper consists of four fingers with two phalanxes, two servo-motors that drive two phalanxes separately, a cable driving system, compliant components, and 120 microspines produced by SDM [154]. Tohoku University developed a rock climbing robot equipping a passive spiny gripper, which is inspired by the digital tendon locking mechanism of *Chiroptera* [155]. The gripper uses a suspension gripping mechanism that can passively and adaptively grasp minor irregularities of rough surfaces without consuming energy. The engagement power is generated by the weight of the robot and passive springs. Its improved version, HubRobo, can complete semiautonomous climbing in a simulated rock climbing environment [156].

Aside from these climbing robots, several attachment devices for climbing robots have been developed. An opposed spiny gripper, developed by Stanford University, enables a quadrotor to perch on vertical and inverted rough walls [157]. It has a higher rigidity and accommodates more spines per unit area than standard spiny robotic toes. The two microspines arrays slide relative to each other on rails separated by a hard stop on the outside of the microspines. Then, the tendon-actuated spring pulls the two sets of microspines inward to complete the attachment when the gripper touches the surface. Stanford University developed a robotic palm

equipped with linearly-constrained spine mechanism [158]. For load-sharing between phalanges, each phalanx is configured with a linearly-constrained spine mechanism operated by cable tendons and sliding within linear guides. The gripper, which was inspired by human rock climbing techniques, can perform various gripping motions, such as pinch grasps or adhering to a structure's border with its fingernails [158]. Stanford University has also developed a manipulator consisting of spiny palm consisting of pneumatic spine array fingers and a particle-jamming pad. The particle-jamming pad can provide compliance to make more spines contact with the irregular surface. With pneumatic force, the microspines can be easily pushed away from the surface and prevented from getting stuck in the slide by small particles. A whiffle tree differential transmission is used for load sharing [159]. Xu et al. [151] developed a four-finger gripper for climbing robots that can stretch and grasp while being powered by an external vehicle-borne pump, as shown in Fig. 17(c). Using the effective stroke of an air cylinder, it can grip the micro-protuberances on a tough wall [151,160]. Guangdong University of Technology developed a soft gripper, as shown in Fig. 17(d) [152], with six claws distributed symmetrically and driven by a shared SMA spring, as well as an elastic composite main body. It adapts well to a wide range of grasping objects and rough surfaces. The claws on both sides of the gripper can generate an effective grasping through forming closure or force closure in different situations [152].

Some climbing robots, such as 3DCLIMBER [161] and Climbot [162], are designed to work on artificial cylindrical structures, such as pipelines, by utilizing grippers. On the contrary, they can hardly adapt to the uneven and intricate natural cylindrical structures such as trees. The Chinese University of Hong Kong's Treebot is the first tree-climbing robot capable of moving up from a tree trunk to a branch with various textures [132,163]. Treebot consists of a continuous maneuvering body and a pair of spiny grippers that can attach to various tree trunks and branches, as shown in Fig. 17(e) [132]. Each claw is made up of two phalanges with a surgical suture needle tip. It employs a two-link mechanism driven by a linear motor to produce the optimal contact force direction. The testing findings suggest that the gripper can withstand 40 N of draw force, which is more than six times the robot's total weight.

5   Sub-ambient pressure adhesion

Some fish and mollusks can use suckers (e.g., octopus suckers, remora suckers, and clingfish suckers) to generate sub-ambient pressure for attachment [110]. Biological suckers generally have better performance of sealing on fouled or irregular attached surfaces than artificial suction cups. The excellent performance of biological suckers can be attributed to two factors: (i) Their structures and actuators are tightly coupled to produce negative pressure via muscle contraction. Little energy is consumed to maintain the sub-ambient pressure because of the unique structures of their internal chamber. (ii) The biological suckers have some special microstructures that can improve their adaptation and produce other adhesion effects, such as wet adhesion and mechanical adhesion, to enhance adhesion and sealing.

5.1   Biological suckers

The octopus, with its flexible, redundantly driven tentacles and highly adaptable suckers, is a suitable representation and emblem of soft robot [3,164]. Octopus suckers can adhere to substrates with various features under water, including rough and smooth surfaces, and they can maintain attachment for an extended period of time while using little muscle energy [164–166]. The amazing function of the octopus sucker is primarily due to its pliable tissues and unusual internal structure [167]. Figure 18(a) [166] illustrates the morphology of an octopus sucker, which has spoke-like grooves, ridges, and a circle of loose tissue on its edge. This structure allows it to adapt to the varying shapes of attached surfaces by expanding and contracting without losing contact to maintain a seal [166]. Figures 18(b) and 18(c) [168] depict the five stages of the octopus sucker's attachment process. The suction cups alter the internal volume by contracting the muscles depicted by the small black arrows, causing a pressure difference between the inside and outside. When all muscles stop contracting, the elastic force (white arrow) is offset by the water's cohesive force (grey arrow). Adhesions, as indicated by the black arrows, impose on the interface between the acetabular roof and wall. Adhesions can be maintained with little energy expenditure [168].

Remoras belonging to *Echeneidae* can easily attach and detach to hosts (e.g., marine animals and ships) with a wide range of roughness using a sucker evolved from the dorsal fin [12,169,170]. As shown in Fig. 19 [12], the unique sucker is formed by integumentary structures and the musculoskeletal system, which includes a soft, flexible disc lip and lamellae with a spinule array arranged in the internal disc. The pectinated bony lamellae can change orientation to help hundreds of microspines on the lamellae engage with asperities. This structure can improve its shear payload capacity [12,170–172]. The erector muscles of the lamellae can generate a sub-ambient pressure differential. With muscle contraction, the internal water volume of the adhesive disc increases, and suction is formed [173]. When the remora detaches from the host, the soft and flexible disc lip curls upward away from the substrate from anterior to posterior of the disc [174].
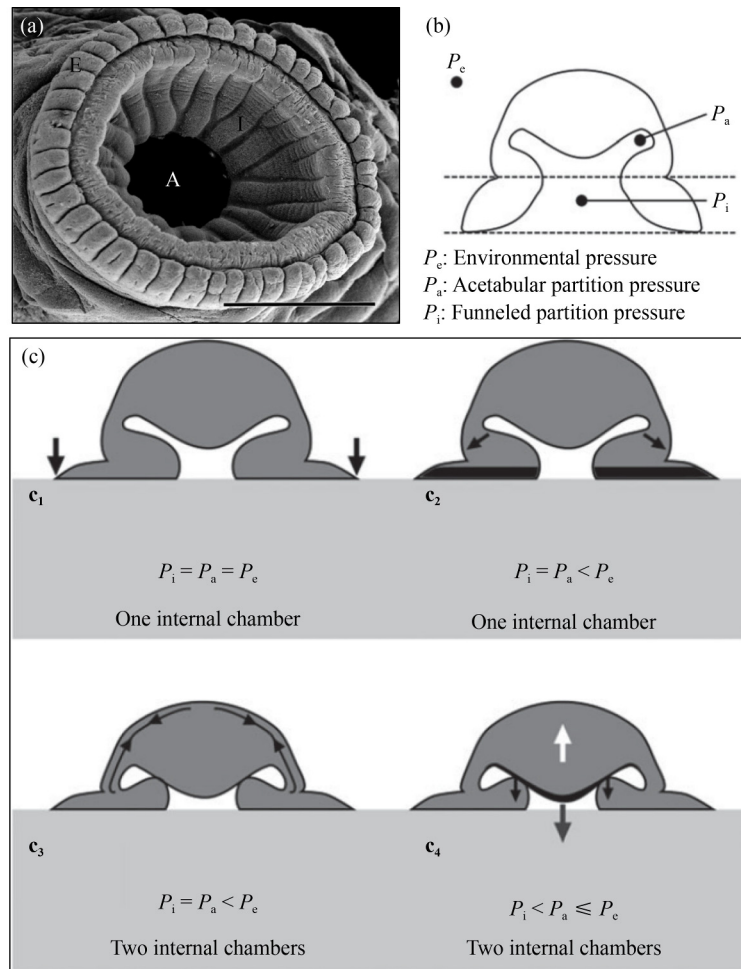
Fig. 18 Morphology and hypothesis adhering process of octopus sucker: (a) scanning electron micrograph of infundibulum of the octopus sucker, reproduced with permission from Ref. [166] from Oxford University Press, (b) internal diagram of octopus sucker, reproduced with permission from Ref. [168] from The Royal Society, and (c) attachment process of the octopus sucker, reproduced with permission from Ref. [168] from The Royal Society.
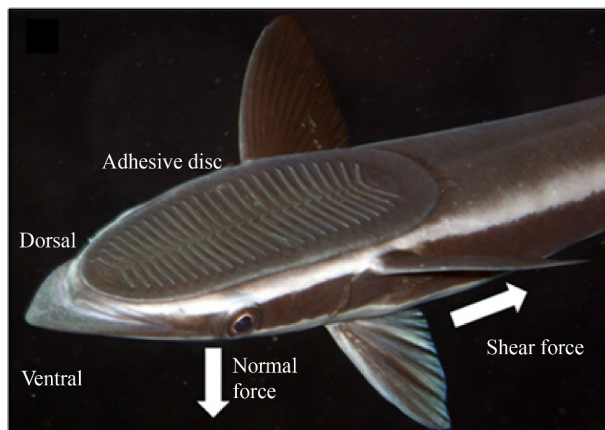
Fig. 19 Morphology of remora disc, reproduced with permission from Ref. [12] from The American Association for the Advancement of Science.

The northern clingfish (*Gobiesox maeandricus*) can generate adhesion of 80 to 230 times its body weight on smooth, contaminative, rugose, or irregular surfaces with a wide range of roughness [175,176]. Figure 20 [176] shows its hierarchical suction disc. The strengthened seal and the composite structure are the key to the northern clingfish's robust adhesion on rough surfaces [177]. On the macroscale, the displacement of the water within clingfish disc can generate sub-ambient pressure to produce adhesion. On the microscale, the microvilli that covered the sucker can conform rough surfaces and maintain a seal during adhesion [22]. Although the clingfish microvilli are similar to those of geckos and arthropods, two evident differences are as follows: (i) The clingfish generates adhesion under water, and (ii) the microvilli around the suction disc lack spatula tips, thereby promoting apical compliance and are crucial for van der Waals force formation [22].

Furthermore, the rock-climbing fish (*Beaufortia kweichowensis*) can crawl on slippery, fouled surfaces using two anisotropic suckers alternately [178]. The suckermouth catfish has evolved some distinctive

Fig. 20 Hierarchical structures from macroscale to microscale of clingfish sucker (*Gobiesox maeandricus*), reproduced with permission from Ref. [176] from The Royal Society, (a) clingfish and its sucker, (b) SEM of the ventral surface of the sucker, (c) SEM 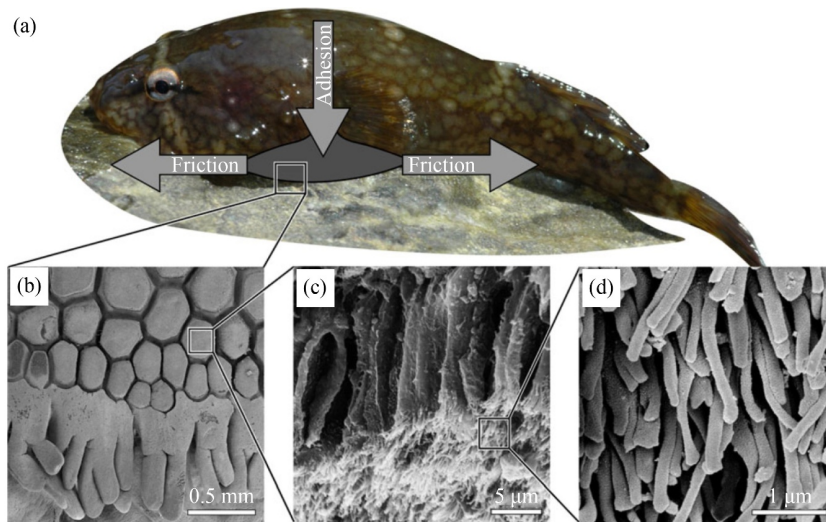of a papilla, consisting of many rods subdivided apically into fibrils, and (d) SEM of the fibrils on the tips of the rod.

characteristics, such as bony armor, a ventral suckermouth, ventrally tilted lower jaws, and muscle configurations that increase jaw mobility [179]. Around the suckermouth, papillae covered with microvilli can increase friction forces [180].

Although some differences are observed among these suckers in morphologies and structures, some similar mechanisms, such as using microstructures to enhance sealing and generating sub-ambient pressure by muscular contraction, can be found in them. Significantly, the microscopic structures, such as spinules, papillae, and microvilli, covering the attachment organs play a key role in maintaining the sub-ambient pressure by promoting the resistance of shear force and sealing.

5.2 Bioinspired suckers

Many artificial suckers are developed with biomimetic structures by taking inspiration from animals as shown in Fig. 21 [12,22,181–184]. Some of them are designed with smart actuators that mimic muscle contractions to generate sub-ambient pressure. Inspired by the octopus, Istituto Italiano di Tecnologia developed an artificial sucker using data of 3D reconstruction of the natural sucker [167] and dielectric elastomer actuators (DEAs) [181]. This sucker is similar in size and adhesion mechanism to a proximal sucker of the octopus; it is composed of an actuation unit held by a plexiglass frame and a silicone-fabricated artificial infundibulum. When the actuator is turned on, the upper film is deformed as shown in Fig. 21(a) [181]. Then, it can generate a decrease in water pressure within the artificial infundibulum. It can generate up to 6 kPa of maximum pressure underwater within 300 ms. Shanghai Jiao Tong University developed two compact suction cup prototypes

inspired by octopus and driven by SMA [182]. A two-way shape memory effect extension TiNi spring is employed to mimic the piston structure in stalked suction cup. However, the sub-ambient pressure cannot be eliminated automatically due to lack of recovery force and friction between inner cylinder and sealing ring. The modified version in Fig. 21(b) [182], which avoids the above disadvantage, is driven by a bias unidirectional SMA actuator. Its basic structure is composed of a stiff margin, a guiding element, a leader, and an elastic element. Tang et al. [185] developed a pneumatic-actuated soft adhesive disc that could work on land and in water and was used in an inchworm-like climbing robot. It is made up of extremely soft bilayer structures with an embedded spiral pneumatic channel resting on top of a cavity-filled base layer. When the spiral pneumatic channel is inflated, the deformation can generate negative pressure [185]. Sholl et al. [186] developed a suction cup with DEA to generate suction inspired by squid and octopus. A Dragon Skin 10 inner core, a VHB 4905 and carbon grease rolled DEA, a Dragon Skin 10 skin, and electrode lead to pressure generation tests comprising the artificial sucker. When activated, the DEA applies electrostatic stress to the end effector's walls, causing pressure to drop in its water-filled cavity. It does not necessitate net fluid flux out of the sucker, allowing rapid attachment and release. Wang et al. [183] developed a magnetically actuated octopus-inspired sucker consisting of an upper layer packed with magnetic particles and a cavity in lower layer, as shown in Fig. 21(c). When a magnetic field is supplied to it, the upper component can deform and affect the pressure of the lower layer.

Mazzolai et al. [184] developed a bionic tentacle, which is driven by three cables and has three types of bionic suction cups shown in Fig. 21(d), to imitate the octopus
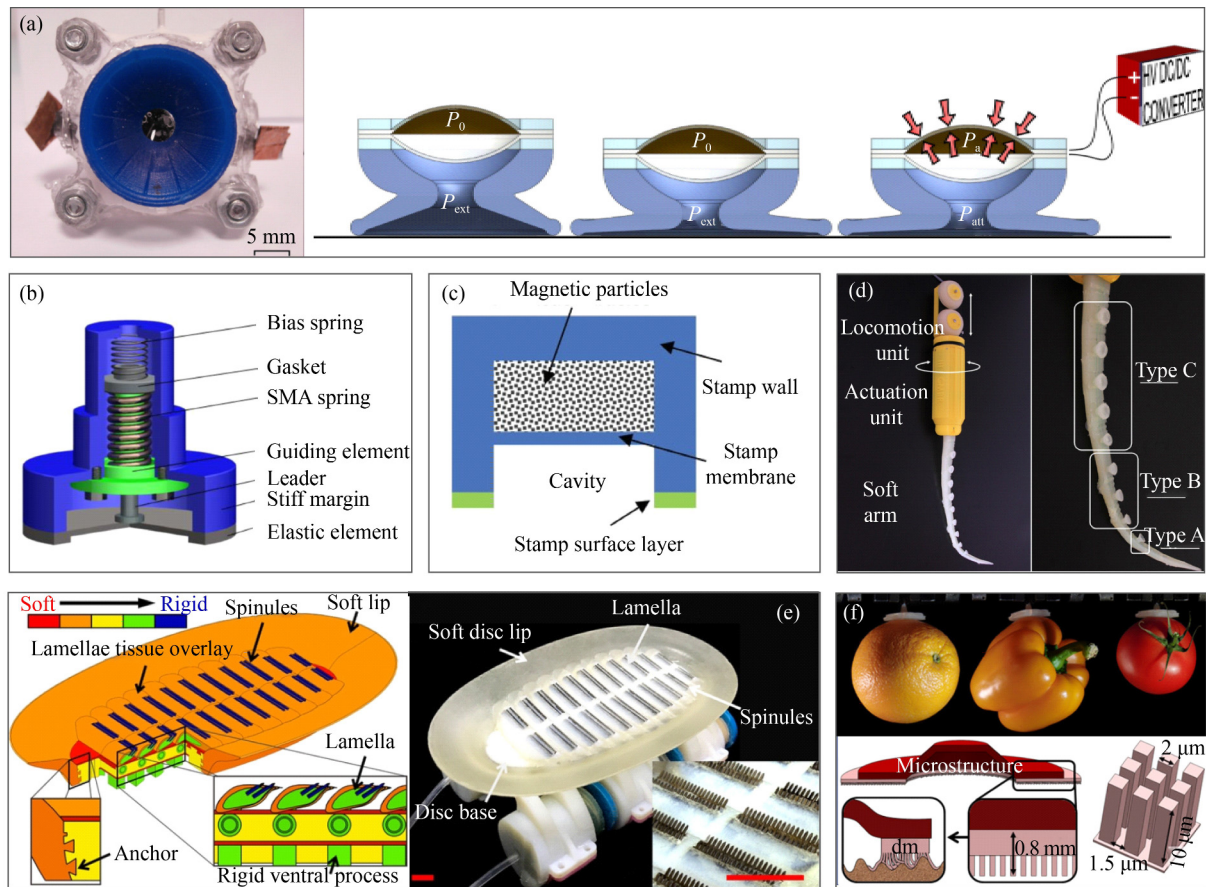
Fig. 21 Bioinspired suction cups: (a) sucker actuated by DEA and its attachment process, reproduced with permission from Ref. [181] from IOP Publishing, (b) CAD model of an octopus-inspired sucker actuated by SMA [182], copyright 2009, (c) magnetically actuated sucker, reproduced with permission from Ref. [183] from John Wiley and Sons, (d) octopus-inspired gripper [184], copyright 2019, (e) remora-like suction disc, reproduced with permission from Ref. [12] from The American Association for the Advancement of Science, and (f) clingfish-inspired sucker, reproduced with permission from Ref. [22] from IOP Publishing.

tentacles. The suction cups are hemispherical in shape, with a flexible stalk at the top that resembles a spherical joint, thereby increasing surface adaptability. The bionic tentacle can attach and grip a wide range of objects in air, water, and oil by winding, adsorption, and external support. Xie et al. [187] incorporated an octopus-like sucker on the surface of the conical soft pneumatic gripper. The conical gripper, as opposed to the columnar gripper, can better adapt to the surfaces of the grasped objects.

Some suction cups are designed to mimic the morphologies and microstructures of animal suction cups. Wang et al. [12] developed a remora-like multimaterial suction disc, as shown in Fig. 21(e). The main disc structure is made by 3D printing to achieve stiffness spanning three orders of magnitude. Carbon fiber is used to make the bionic spinules using laser machining techniques. Electrostatic flocking is used to embed vertically oriented nylon fibers into the soft silicone matrix in the disc, which is inspired by the tissue of the remora disc [187]. When the disc is twisted, the stiff spinules and soft material covering on the lamellae can engage with the surface, increasing the shearing load capability [12,174].

Ditsche and Summers [177] developed a bionic suction cup that mimics the material properties of the rigid−flexible coupling of the clingfish sucker and the microstructure of its outer edge. This design can increase friction, delay failure, and allow the sucker to adhere to rough surfaces. A bioinspired suction disc developed by Sandova et al. [22] is lined with microscopic silicone pillars that mimic the fibrils on the papillae of the clingfish disc shown in Fig. 21(f) to improve sealing performance. This suction disc adheres and seals better than ordinary artificial suction cups on rough surfaces [22].

6   Summary and discussion

This section provides a summary of bioinspired attachment device design methods, with a focus on the design and control of climbing robots using bioinspired attachment, as shown in Fig. 22. The difficulties
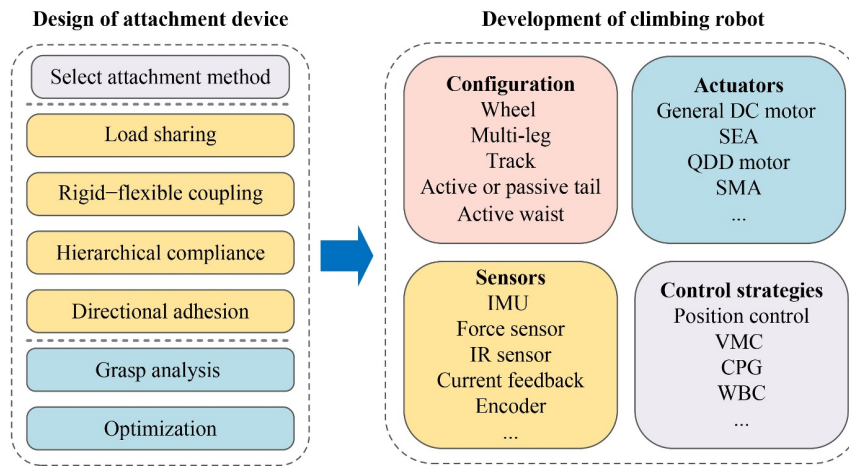
Fig. 22   Methods for developing bioinspired attachment devices and bioinspired climbing robots.

encountered and perspectives in the application of bioinspired attachments in robotics are also discussed.

6.1   Bioinspired adhesion devices

The appropriate adhesive method should be to select based on the usage scenario. If the attached surface is flat and in air, then suction cups should be used, and bionic microstructure can improve their performance. Bioinspired dry adhesives can be used for adhesion on smooth or non-airy surfaces. Mechanical adhesion is suitable for use on surfaces with millimeter- or centimeter-level roughness. Magnet adhesion is preferred for attachment on ferromagnetic surfaces. Wet adhesion is a technique for attaching to wet, slippery surfaces. Bioinspired suction cups can generate negative pressure through internal deformation and can thus be used to attach to flat surfaces underwater or in the air.

According to the above survey on bioinspired attachment devices, we can propose the following universal design methods:

(1) Load-sharing [159,188]. The overall load is distributed into as many adhesive units as possible to avoid part overload or attachment system failure. Load-sharing attachment systems can also reduce internal stress between different components. It can be accomplished through flexible deformation of adhesive units, or through the use of mechanisms, such as movable pulleys and seesaw mechanisms to connect different parts of adhesive units for load-sharing.

(2) Rigid−flexible coupling and hierarchical compliance [19,80,188]. The attachment system should be configured with multilevel compliance to conform to the surface shape and to increase contact area. Biological attachment devices are made up of flexible and rigid components, such as muscles, tendons, and skins, as well as skeletons and keratinous structures. When structures with very different stiffnesses are combined, stress concentrations emerge at the interface, thereby causing

fracture or failure [17]. Rigid−flexible coupling design and additive manufacturing, such as SDM and multimaterial 3D printing are used to effectively combine soft materials with hard structural components.

(3) Directional adhesion [17]. Adhesive systems should generate appropriate adhesion with robust attachment and easy detachment; thus, attachment and detachment in a specific route is an option. The motion planning and locomotion mechanism design of robots should be matched with the asymmetric features of adhesive pads for easy attachment and detachment. For microspines, the optimal approach vector to contact with the rough surface should be used so that spine tips can easily interlock with asperities and depart from the surface with minimal disturbance. It is typically obtained through theoretical simulations and experiments.

Furthermore, wrench workspaces of attachment devices should be calculated and described to optimize their design and select the best grasping method for each task.

6.2   Focus on bionic climbing robot

6.2.1   Adhesive system and configuration

Dry adhesion, wet adhesion, and mechanical adhesion, which are exploited by climbing animals to attach, are naturally suitable for applications in climbing robots. Although many types of artificial wet adhesives are developed in recent years [120,189,190], only few applications on robotics are reported [104,125]. The automatic mucus secretion devices and controllable adhesion methods are difficult to achieve at present; thus, wet adhesion is hardly applied in robot. Bioinspired suction cups are more suitable for static attachment in the gripper of robots and autonomous underwater vehicles (AUVs) than for dynamic climbing. Some robots use claws and adhesive pads to adapt to more surfaces [100,135,191], similar to the way insects attach [134]. Some robots can also change attachment devices for

attaching to surfaces with different characteristics [25,192].

According to Tables 1 [24,53−55,80−83,85,86,90−92, 193] and 2 [18,19,25,132,139,141,143,144,146−149,194, 195], the majority of climbing robots in use is lightweight and small because the active area of their attachment devices cannot keep up with the weight growth as the robot grows [105]. Moreover, large attachment devices are more prone to undergo stress concentrations, which can lead to attachment failure [196]. Climbing robots that use wheels or tracks to move would perform better in terms of body length per second moved (BL). Robots with more complex movement mechanisms can better adapt to changes in terrain, but their climbing speed suffers as a result.

Toes on wheeled climbing robots always use adhesive pads or microspines for attachment and movement. They are required to support the body weight of the robot to maintain continuous contact between the toes and the attached surface. Each toe should be flexible sufficiently to adjust to the terrain and return to a neutral posture. Climbing robots with wheels and tracks frequently have a tail or an active waist to provide preload to avoid overturn.

To assure stability, most legged climbing robots use static gaits, which require at least three feet in stance. The limbs and feet of the legged climbing robots are always constructed with a multilevel compliant system and some passive DOFs to adapt to the attached surface. Some unique planar linkage mechanisms are applied in the bioinspired climbing robots to generate a suitable foot trajectory to simplify the leg structure and minimize the weight of the robot. Four-bar linkage mechanism is frequently employed to the legs of climbing robots [18,81,197,198]. However, reducing the number of DOFs reduces the robot's flexibility and terrain adaptability. These robots can usually only climb on flat surfaces by specific gaits. Climbing robots, whether in body or limbs, have not yet reached the compliance and agility of climbing animals. The addition of a preloaded tail can help the climbing robot balance the turning moment [92]. If the turning moment caused by gravity and normal forces can be balanced by limbs, then a tail is unnecessary [143].

6.2.2 Actuators and sensors

Many researchers employ servo motors as joint actuators of climbing robots. The servo is a type of modular robotic

Table 1 Typical climbing robots with dry adhesives

Reference	Weight/g	Size/mm	Climbing angle and surface	Speed/ (mm·s⁻¹)	BL/s	Configuration	Attachment device
Geckobot [82]	100.0	$L = 190.00$, $W = 110.00$	85° and acrylic surface	10.00	0.053	Four legs driven by linkage, six motors and an active tail	Gecko-like PDMS adhesive pad driven by tendons
Stickybot [24]	370.0	$L = 600.00$, $W = 200.00$, $H = 60.00$	90° and glass, tile, acrylic, polished granite	40.00	0.067	A flexible body, four legs, 12 motors, and a passive tail	Gecko-like PU anisotropic adhesive pads driven by tendons
CLASH [85]	19.0	$L = 100.00$	75° and acrylic surface	100.00	1.000	Six legs, a motor, and a scaled smart composite microstructure constructed body	RCM ankle and a wedge-shape PDMS adhesive pad
Abigaille II [86]	260.0	$D = 90.00$	90° and PMMA	1.00	0.011	Six legs with three active DOFs	MSAMS PDMS adhesive pads
Abigaille-III [80]	634.6	$L = 200.00$, $W = 210.00$, $H = 90.00$	90° and PMMA	0.44	0.002	Six legs with four active DOFs	MSAMS PDMS adhesive pads
AnyClimb II [81]	138.0	$L = 140.00$, $W = 120.00$, $H = 49.00$	90° and acrylic surface	12.50	0.089	Eight legs, a steering mechanism with a motor and two bevel gears, and a passive tail	Vytaflex-10 flat adhesive pads
UNIclimb [83]	363.0	$L = 230.00$, $W = 200.00$, $H = 55.00$	180° and glass	14.00	0.061	Four legs with three active DOFs	Multilayered footpad with MSAMS adhesives and SiO_2-F hydrophobic coating
Gecko robot_7 [55]	700.0	$L = 400.00$, $W = 260.00$, $H = 80.00$	180° and glass surface	1.70	0.004	Four legs with three active DOFs	Feet with four MSAMS PVS adhesive pads driven by tendon
Gecko-like robot [193]	1980.0	$L = 440.00$, $W = 260.00$	90° and glass and Teflon	6.00	0.014	Four legs with three active DOFs	PVS MSAMS adhesive pad
Waalbot II [90]	85.0	$L = 95.60$	180° and glass, acrylic, and wood	50.00	0.523	Two whegs, two motors, a passive joint in the pivot, and two passive tails	Whegs with three MSAMS PU adhesive pads and passively peeling ankles
Mini-Whegs [54]	21.8	$L = 47.00$	180° and glass	85.00	1.805	Two whegs, a single motor, and a passive tail	Whegs with four MSAMS PVS adhesive pads
Orion [91]	71.5	$L = 59.04$, $H = 34.90$	180° and acrylic surface	30.00	0.508	Two whegs, a single motor, and a passive tail	Whegs with bilayer adhesive pads made by PDMS and 3M VHB tape
Tankbot [92]	115.0	$L = 190.00$	180° and wooden door, glass	120.00	0.632	Two tracks, a motor, and an active tail	Vytaflex-10 adhesive tracks
TBCP-II [53]	240.0	$L = 215.00$, $W = 200.00$	90° and PMMA, glass and painted steel	34.00	0.158	Four actuated tracks and an active waist	MSAMS adhesive tracks made by PDMS

Notes: L, body length; H, body height; W, body width; PMMA, Polymethyl methacrylate.

Table 2 Typical climbing robots with microspines

Reference	Weight/g	Size/mm	Climbing angle and surface	Speed/ (mm·s⁻¹)	BL/s	Configuration feature	Attachment device
Spinybot II [139]	400	N/A	90° and rough wall	23.00	0.053	Six legs, seven servo motors, and a passive tail	Toe with spine mechanism fabricated by SDM
RiSE V2 [18]	3800	$L = 600$	90° and rough wall	40.00	0.067	Six legs with two active DOFs and an active tail	Toe with spine mechanism fabricated by SDM
ROCR [194]	550	$L = 460$	90° and rough wall	157.00	0.340	A pendulum-like tail and a main body with two claws	Steel claws
CLIBO [143]	2000	$L = 750$	90° and rough wall	60.00	0.080	Four legs with four DOFs	Toes with steel claws
DynoClimber [146]	2600	$L = 400$, $W = 116$, $H = 70$	90° and textile wall	670.00	1.675	Two four-bar linkage arms driven by a motor	Toes with spine mechanism fabricated by SDM
BOB 2.0 [144]	300	Length of leg: 200	90° and textile wall	250.00	1.250	Two arms, a motor, and a passive tail	Toes with spine mechanism fabricated by SDM
BOBCAT [195]	5000	$L = 600$	90° and textile wall	170.00	0.283	Four five-bar legs with two active DOFs	Toes with spine mechanism fabricated by SDM
Wall climbing robot [194]	400	$L = 480$, $W = 240$, $H = 30$	90° and board	46.00	0.096	A body and four four-bar legs with two active DOFs	Flexible rubber pads with claws
Soft climbing robot [147]	37	$L = 120$, $W = 124$, $H = 42$	90° and rough wall	2.00	0.017	An SMA driven body and two spiny feet	PDMS feet with steel microspines
SpinyCrawler [148]	208	$L = 242$, $W = 124$, $H = 42$	180° and rough wall	18.00	0.074	A spiny track driven by a motor and two compliant tails	Spiny tracks
Tbot [141]	60	$L = 120$, $W = 110$	100° and rough wall	100.00	0.833	Two wheels, a motor, and a passive tail	Spiny wheels printed by nylon
TriDROP [149]	394	$L = 470$, $W = 220$, $H = 100$	90° and rough wall	300.00	0.638	Three wheels and an active waist	Spiny wheels made by SDM
Treebot [132]	600	$L = 325$, $W = 175$, $H = 135$	105° and tree trunk	300.00	0.004	Two spiny grippers and continuum body	Passive spiny gripper with four fingers
LEMUR IIB [19]	N/A	N/A	105° and rock	N/A	N/A	Four legs with active three DOFs	Spiny grippers with 16 fingers and four DC motors
LEMUR 3 [25]	35000	N/A	N/A and cliff face	0.04	N/A	Four legs with seven active DOFs	Spiny grippers with 16 fingers and four DC motors
Free-climbing robot [132]	1600	$W = 1600$, $H = 130$	90° and artificial rock face with 1/3 gravity	2.83	1.805	Four legs with three active DOFs	Passive spiny gripper with six fingers and a motor for detaching

Notes: N/A, not available; L, body length; H, body height; W, body width.

joint that can be easily assembled. It generally consists of a direct current (DC) motor, reducer with a high reduction ratio, a driver, sensors, shells, and some other components. In general, it can satisfy the climbing robot's dynamic performance and real-time communication requirements. However, most servos can only be used in the position mode, and the torque mode is difficult to use. Based on the designs of multilegged robots, quasi-direct drive (QDD) joints and serial elastic actuators (SEAs), which can be precisely modeled and controlled for output torque, have prospective applications in the field of bioinspired climbing robots.

Distance sensors, force sensors, and inertial measurement units (IMUs) are often employed in climbing robots. Ultrasonic and IR sensors are common distance sensors used in bioinspired climbing robots that can enable the robots to acquire distance feedback from the attached surfaces and information of environments [53,80]. Force sensors provide feedback to robots during touchdown and can be used to adjust the adhesion force [24]. Alternatively, the robot can calculate the output force directly from the motor torque [143]. IMU can provide robots with orientation and velocity feedback to estimate their states [156]. Vision sensors and LiDAR are less prevalent due to the small size and the limited onboard computing capacity of most bioinspired climbing robots. The lack of vision limits the observation and decision-making abilities of robots; therefore, these robots are generally poor in automation and adaptation to environmental changes.

6.2.3 Control strategies

Most current control algorithms of climbing robots are based on kinematics models, owing to their low movement rates, quasi-static states, and dynamic performance. Furthermore, the transmission ratios of actuators utilized in most climbing robots are very high; thus, simulating nonlinear parts in dynamics, such as viscous friction, is challenging. On the contrary, the lack of joint torque regulation, hinders the climbing robot from executing dynamic animal-like climbing and from modulating the required attachment force of each foot. By observing the climbing motion of a cockroach, Goldman et al. [199] established a dynamic climbing model, which adds springs and linear actuators between the robot's center of mass and attachment point. It is similar to the spring-loaded inverted pendulum model of multilegged

robots [200] and has been applied to some robots for dynamic climbing motion control (e.g., BOB 2.0 [144], Dyno-Climber [146]). Stickybot achieves contact force modulation by modeling the limbs with spring damping and collecting force feedback with force sensors. Such models neglect the mass of the limbs and are hence inapplicable to many mechanisms of climbing robots. The whole-body control (WBC) [201] may be applied to climbing robot in the future. Virtual model control (VMC) or hybrid position and force control can be used to regulate the desired support reaction force of the body. Central pattern generator (CPG) can also be used in the gait generation of climbing robots [202]. CPG usually generates movements of individual joints by simulating the spinal nerve signals of animals and modulates these movements through reflexes.

6.3 Challenges and perspectives

As a highly interdisciplinary field, bioinspired attachment technologies have considerable potentials but also have some challenges. In previous sections, the limitations of current studies for each type of bioinspired attachment method were discussed. Some challenges for bioinspired attachment applications in robots are as follows:

(i) Contrary to animals, no hardware structures come close to the level of integration of sensing, actuation, and energy supply found in living organisms. Muscle-like actuators with contraction and transformation functions, such as SMA and DEA, lack robustness, efficiency, and energy and power density [203].

(ii) As robots venture beyond the laboratory, models of real-world, unstructured environments will be required, but none can adequately represent our complex and ever-changing world. The interaction between the climbing robot and the environment, in particular, is a time-varying system with a highly nonlinear and strong coupling dynamic model.

(iii) Robots have greater gap than animals in flexibility due to lack of sufficient active joints. Robots require high compliance to adapt to the surface to which they are attached, but at the same time, they require high stiffness to achieve high positional accuracy. This finding may seem very contradictory, but its essence is because control and sensing systems of robots cannot match with the powerful neural systems of living beings.

(iv) Attachment devices have a short lifespan nowadays, limiting their use in robotics. In the future, novel designs and manufacturing techniques of multifunctional materials should be used in attachment devices to improve material strength, stiffness, flexibility, fracture toughness, wear resistance, and energy absorption.

Bioinspired attachment technologies can be widely used in the robotics field in the future. Space capture devices can be equipped with dry adhesive grippers as their end effectors to catch space debris; they are more effective than the present space capture devices. Reversible wet adhesive pads have the potential to be applied in wearable devices, climbing robots, AUVs, and drug delivery facilities [110]. Bioinspired suckers can provide solutions for AUVs to hitchhike [12,204], collecting specimens underwater [186], robot end-effectors, and climbing robot attachment devices. Mechanical adhesive devices can be used not only in climbing robots, but also in other mobile robots (e.g., jumping robot [135], biped robot [205]), and drilling equipment [19].

7 Conclusions

For living in various and complex environments, many organisms have evolved unique organs for excellent functions, such as adhesion, climbing, and predation. These natural outcomes are based on multiple attachment mechanisms from nanoscale to macroscale. Herein, we divide the reversible biological attachment methods exploited into four categories: dry adhesion, wet adhesion, mechanical adhesion, and sub-ambient pressure adhesion. Biological attachment methods are explained in terms of their corresponding morphologies, mechanism of adhesion, and models of adhesion. The characteristics, mechanical structures, design ideas, and fabrication methods of typical bioinspired attachment devices of each attachment type are introduced. Furthermore, the limitations and challenges of the current bioinspired adhesive research are discussed. The application situations and design principles of the bioinspired attachment methods are summarized. The climbing robots that use adhesives and mechanical adhesion are reviewed, including their configurations, performance, and mechanical designs.

Nomenclature

Abbreviations

AR	Aspect ratio
AUV	Autonomous underwater vehicle
BL	Body length per second moved
CPG	Central pattern generator
DC	Direct current
DEA	Dielectric elastomer actuator
DOF	Degree of freedom
IMU	Inertial measurement unit
IR	Infrared ray
JPL	Jet Propulsion Laboratory
MSAMS	Mushroom-shaped adhesive microstructure

26   Front. Mech. Eng. 2022, 17(3): 43

PDMS   Polydimethylsiloxane

PMMA   Polymethyl methacrylate

PS   Polystyrene

PU   Polyurethane

PUA   Polyurethane acrylate

PVS   Polyvinyl siloxane

QDD   Quasi-direct drive

RCM   Remote center-of-motion

SDM   Shape deposition manufacturing

SEA   Serial elastic actuator

SMA   Shape memory alloy

VMC   Virtual model control

WBC   Whole-body control

Variables

A Hamaker constant

d Normalized separation in the multiple wet adhesion model

D Separation distance between the two surfaces

f Normalized total force in the multiple wet adhesion model

F Shear force along the attached substrate in Fig. 13(a)

F_a Force per area between two planar surfaces in van der Waals force model

F_{cap} Capillarity force

F_{hyd} Hydrodynamic force

F_n Multiple wet adhesion

h Height of the liquid film

h_{asp} Depth of the center of the asperity as shown in Fig. 13(a)

n Number of small drops

r_s Radius of the microspine

r_{tip} Radius of the claw tip

R Radius of the contact unit in wet adhesion model

R_{asp} Radius of the asperity in Fig. 13(a)

s Scale factor in the multiple wet adhesion model

t Separating time of the two surfaces in wet adhesion model

V Volume of one large liquid droplet

W Weight acting on the claw directed normal of the attached surface

α Angle as shown in Fig. 13(a)

θ_1, θ_2 Contact angles of the liquid film with contact unit and the surface respectively in Fig. 8

θ_{load} Angle between the surface and the direction of external force

θ_{min} Critical attachment angle between the attached surface and the claw

γ Surface tension

η Liquid viscosity

μ Friction coefficient between claw end and attached surface

Acknowledgements   This work was financially supported by the National Key R&D Program of China (Grant No. 2019YFB1309600), and the National Natural Science Foundation of China (Grant Nos. 51775011 and 91748201).

Open Access   This article is licensed under a Creative Commons Attribution 4.0 International License, which permits use, sharing, adaptation, distribution, and reproduction in any medium or format as long as appropriate credit is given to the original author(s) and source, a link to the Creative Commons license is provided, and the changes made are indicated.

The images or other third-party material in this article are included in the article's Creative Commons license, unless indicated otherwise in a credit line to the material. If material is not included in the article's Creative Commons license and your intended use is not permitted by statutory regulation or exceeds the permitted use, you will need to obtain permission directly from the copyright holder.

Visit http://creativecommons.org/licenses/by/4.0/ to view a copy of this license.

References

1. Autumn K, Liang Y A, Hsieh S T, Zesch W, Chan W P, Kenny T W, Fearing R, Full R J. Adhesive force of a single gecko foot-hair. Nature, 2000, 405(6787): 681–685

2. Autumn K, Sitti M, Liang Y A, Peattie A M, Hansen W R, Sponberg S, Kenny T W, Fearing R, Israelachvili J N, Full R J. Evidence for van der Waals adhesion in gecko setae. Proceedings of the National Academy of Sciences of the United States of America, 2002, 99(19): 12252–12256

3. Tramacere F, Kovalev A, Kleinteich T, Gorb S N, Mazzolai B. Structure and mechanical properties of Octopus vulgaris suckers. Journal of the Royal Society Interface, 2014, 11(91): 20130816

4. Dai Z D, Gorb S N, Schwarz U. Roughness-dependent friction force of the tarsal claw system in the beetle Pachnoda marginata (Coleoptera, Scarabaeidae). Journal of Experimental Biology, 2002, 205(16): 2479–2488

5. Voigt D, de Souza E J, Kovalev A, Gorb S. Inter- and intraspecific differences in leaf beetle attachment on rigid and compliant substrates. Journal of Zoology, 2019, 307(1): 1–8

6. Gorb S N. Biological attachment devices: exploring nature's diversity for biomimetics. Philosophical Transactions of the Royal Society A: Mathematical Physical and Engineering Sciences, 2008, 366(1870): 1557–1574

7. Arzt E, Gorb S, Spolenak R. From micro to nano contacts in biological attachment devices. Proceedings of the National Academy of Sciences of the United States of America, 2003, 100(19): 10603–10606

8. Kesel A B, Martin A, Seidl T. Adhesion measurements on the attachment devices of the jumping spider Evarcha arcuata. Journal of Experimental Biology, 2003, 206(16): 2733–2738

9. Niederegger S, Gorb S N. Friction and adhesion in the tarsal and metatarsal scopulae of spiders. Journal of Comparative Physiology A, 2006, 192(11): 1223–1232

10. Gasparetto A, Seidl T, Vidoni R. A mechanical model for the adhesion of spiders to nominally flat surfaces. Journal of Bionics Engineering, 2009, 6(2): 135–142

11. Barnes W J P. Functional morphology and design constraints of

smooth adhesive pads. MRS Bulletin, 2007, 32(6): 479–485

12. Wang Y P, Yang X B, Chen Y F, Wainwright D K, Kenaley C P, Gong Z Y, Liu Z M, Liu H, Guan J, Wang T M, Weaver J C, Wood R J, Wen L. A biorobotic adhesive disc for underwater hitchhiking inspired by the remora suckerfish. Science Robotics, 2017, 2(10): eaan8072

13. Li J, Gao X S, Fan N J, Li K J, Jiang Z H, Jiang Z J. Adsorption performance of sliding wall-climbing robot. Chinese Journal of Mechanical Engineering, 2010, 23(6): 733–741

14. Gao Y, Wei W, Wang X M, Li Y J, Wang D L, Yu Q D. Feasibility, planning and control of ground-wall transition for a suctorial hexapod robot. Applied Intelligence, 2021, 51(8): 5506–5524

15. Geissmann L, Denuder M, Keusch D, Pfirter L, Röthlisberger D, Ritter M, Thoma P, Siegwart R, Fischer W, Caprari G, Weber J, Beardsley P. Paraswift—a hybrid climbing and base jumping robot for entertainment, In: Bidaud P, Tokhi M O, Grand C, Virk G S, eds. Field Robotics. Paris: World Scientific, 2012, 397–406

16. Schmidt D, Berns K. Climbing robots for maintenance and inspections of vertical structures—a survey of design aspects and technologies. Robotics and Autonomous Systems, 2013, 61(12): 1288–1305

17. Kim S, Spenko M, Trujillo S, Heyneman B, Mattoli V, Cutkosky M R. Whole body adhesion: hierarchical, directional and distributed control of adhesive forces for a climbing robot. In: Proceedings of 2007 IEEE International Conference on Robotics and Automation. Rome: IEEE, 2007, 1268–1273

18. Spenko M J, Haynes G C, Saunders J A, Cutkosky M R, Rizzi A A, Full R J, Koditschek D E. Biologically inspired climbing with a hexapedal robot. Journal of Field Robotics, 2008, 25(4–5): 223–242

19. Parness A, Frost M, Thatte N, King J P, Witkoe K, Nevarez M, Garrett M, Aghazarian H, Kennedy B. Gravity-independent rock-climbing robot and a sample acquisition tool with microspine grippers. Journal of Field Robotics, 2013, 30(6): 897–915

20. Chu Z Y, Wang C, Hai X, Deng J, Cui J, Sun L N. Analysis and measurement of adhesive behavior for gecko-inspired synthetic microwedge structure. Advanced Materials Interfaces, 2019, 6(12): 1900283

21. Wang Z Z. Slanted functional gradient micropillars for optimal bioinspired dry adhesion. ACS Nano, 2018, 12(2): 1273–1284

22. Sandoval J A, Jadhav S, Quan H, Deheyn D D, Tolley M T. Reversible adhesion to rough surfaces both in and out of water, inspired by the clingfish suction disc. Bioinspiration & Biomimetics, 2019, 14(6): 066016

23. Yang X, Tan R, Lu H J, Shen Y J. Starfish inspired milli soft robot with omnidirectional adaptive locomotion ability. IEEE Robotics and Automation Letters, 2021, 6(2): 3325–3332

24. Kim S, Spenko M, Trujillo S, Heyneman B, Santos D, Cutkosky M R. Smooth vertical surface climbing with directional adhesion. IEEE Transactions on Robotics, 2008, 24(1): 65–74

25. Parness A, Abcouwer N, Fuller C, Wiltsie N, Nash J, Kennedy B. LEMUR 3: A limbed climbing robot for extreme terrain mobility in space. In: Proceedings of 2017 IEEE International Conference on Robotics and Automation. Singapore: IEEE, 2017, 5467–5473

26. Santos D, Heyneman K, Kim S, Esparza N, Cutkosky M R. Gecko-inspired climbing behaviors on vertical and overhanging surfaces. In: Proceedings of 2008 IEEE International Conference on Robotics and Automation. Pasadena: IEEE, 2008, 1125–1131

27. Lam T L, Xu Y S. Climbing strategy for a flexible tree climbing robot-treebot. IEEE Transactions on Robotics, 2011, 27(6): 1107–1117

28. Arzt E, Gorb S, Spolenak R. From micro to nano contacts in biological attachment devices. Proceedings of the National Academy of Sciences of the United States of America, 2003, 100(19): 10603–10606

29. Ji A H, Han L B, Dai Z D. Adhesive contact in animal: morphology, mechanism and bio-inspired application. Journal of Bionics Engineering, 2011, 8(4): 345–356

30. Israelachvili J N. Intermolecular and Surface Forces. 3rd ed. Washington: Academic Press, 2011

31. Tian Y, Pesika N, Zeng H B, Rosenberg K, Zhao B X, McGuiggan P, Autumn K, Israelachvili J. Adhesion and friction in gecko toe attachment and detachment. Proceedings of the National Academy of Sciences of the United States of America, 2006, 103(51): 19320–19325

32. Majidi C, O'Reilly O M, Williams J A. On the stability of a rod adhering to a rigid surface: shear-induced stable adhesion and the instability of peeling. Journal of the Mechanics and Physics of Solids, 2012, 60(5): 827–843

33. Autumn K, Peattie A M. Mechanisms of adhesion in geckos. Integrative and Comparative Biology, 2002, 42(6): 1081–1090

34. Autumn K. Gecko adhesion: structure, function, and applications. MRS Bulletin, 2007, 32(6): 473–478

35. Kwak J S, Kim T W. A review of adhesion and friction models for gecko feet. International Journal of Precision Engineering and Manufacturing, 2010, 11(1): 171–186

36. Chen B, Wu P D, Gao H. Hierarchical modelling of attachment and detachment mechanisms of gecko toe adhesion. Proceedings of Royal Society A: Mathematical, Physical and Engineering Sciences, 2008, 464(2094): 1639–1652

37. Federle W. Why are so many adhesive pads hairy? Journal of Experimental Biology, 2006, 209(14): 2611–2621

38. Hansen W R, Autumn K. Evidence for self-cleaning in gecko setae. Proceedings of the National Academy of Sciences of the United States of America, 2005, 102(2): 385–389

39. Hu S H, Lopez S, Niewiarowski P H, Xia Z H. Dynamic self-cleaning in gecko setae via digital hyperextension. Journal of the Royal Society Interface, 2012, 9(76): 2781–2790

40. Xu Q, Wan Y Y, Hu T S H, Liu T X, Tao D S, Niewiarowski P H, Tian Y, Liu Y, Dai L M, Yang Y Q, Xia Z H. Robust self-cleaning and micromanipulation capabilities of gecko spatulae and their bio-mimics. Nature Communications, 2015, 6(1): 8949

41. Li Y S, Krahn J, Menon C. Bioinspired dry adhesive materials and their application in robotics: a review. Journal of Bionic Engineering, 2016, 13(2): 181–199

42. Autumn K, Dittmore A, Santos D, Spenko M, Cutkosky M. Frictional adhesion: a new angle on gecko attachment. Journal of Experimental Biology, 2006, 209(18): 3569–3579

43. Gravish N, Wilkinson M, Autumn K. Frictional and elastic energy in gecko adhesive detachment. Journal of the Royal Society Interface, 2008, 5(20): 339–348

44. Hensel R, Moh K, Arzt E. Engineering micropatterned dry adhesives: from contact theory to handling applications. Advanced Functional Materials, 2018, 28(28): 1800865

45. Wang W, Liu Y, Xie Z W. Gecko-like dry adhesive surfaces and their applications: a review. Journal of Bionics Engineering, 2021, 18(5): 1011–1044

46. Spolenak R, Gorb S, Arzt E. Adhesion design maps for bio-inspired attachment systems. Acta Biomaterialia, 2005, 1(1): 5–13

47. Geim A K, Dubonos S V, Grigorieva I V, Novoselov K S, Zhukov A A, Shapoval S Y. Microfabricated adhesive mimicking gecko foot-hair. Nature Materials, 2003, 2(7): 461–463

48. Sitti M, Fearing R S. Synthetic gecko foot-hair micro/nano-structures as dry adhesives. Journal of Adhesion Science and Technology, 2003, 17(8): 1055–1073

49. Glassmaker N J, Jagota A, Hui C Y, Kim J. Design of biomimetic fibrillar interfaces: 1. making contact. Journal of the Royal Society Interface, 2004, 1(1): 23–33

50. Hui C Y, Glassmaker N J, Tang T, Jagota A. Design of biomimetic fibrillar interfaces: 2. mechanics of enhanced adhesion. Journal of the Royal Society Interface, 2004, 1(1): 35–48

51. Murphy M P, Aksak B, Sitti M. Gecko-inspired directional and controllable adhesion. Small, 2009, 5(2): 170–175

52. Sameoto D, Menon C. A low-cost, high-yield fabrication method for producing optimized biomimetic dry adhesives. Journal of Micromechanics and Microengineering, 2009, 19(11): 115002

53. Krahn J, Liu Y, Sadeghi A, Menon C. A tailless timing belt climbing platform utilizing dry adhesives with mushroom caps. Smart Materials and Structures, 2011, 20(11): 115021

54. Breckwoldt W A, Daltorio K A, Heepe L, Horchler A D, Gorb S N, Quinn R D. Walking inverted on ceilings with wheel-legs and micro-structured adhesives. In: Proceedings of 2015 IEEE/RSJ International Conference on Intelligent Robots and Systems. New York: IEEE, 2015, 3308–3313

55. Yu Z W, Shi Y, Xie J X, Yang S X, Dai Z D. Design and analysis of a bionic adhesive foot for gecko robot climbing the ceiling. International Journal of Robotics and Automation, 2018, 33(4): 445–454

56. Parness A, Soto D, Esparza N, Gravish N, Wilkinson M, Autumn K, Cutkosky M. A microfabricated wedge-shaped adhesive array displaying gecko-like dynamic adhesion, directionality and long lifetime. Journal of the Royal Society Interface, 2009, 6(41): 1223–1232

57. Jiang H, Hawkes E W, Fuller C, Estrada M A, Suresh S A, Abcouwer N, Han A K, Wang S Q, Ploch C J, Parness A, Cutkosky M R. A robotic device using gecko-inspired adhesives can grasp and manipulate large objects in microgravity. Science Robotics, 2017, 2(7): eaan4545

58. Alizadehyazdi V, Bonthron M, Spenko M. An electrostatic/gecko-inspired adhesives soft robotic gripper. IEEE Robotics and Automation Letters, 2020, 5(3): 4679–4686

59. Hossfeld C K, Schneider A S, Arzt E, Frick C P. Detachment behavior of mushroom-shaped fibrillar adhesive surfaces in peel testing. Langmuir, 2013, 29(49): 15394–15404

60. Heepe L, Kovalev A E, Filippov A E, Gorb S N. Adhesion failure at 180000 frames per second: direct observation of the detachment process of a mushroom-shaped adhesive. Physical Review Letters, 2013, 111(10): 104301

61. del Campo A, Greiner C, Alvarez I, Arzt E. Patterned surfaces with pillars with controlled 3D tip geometry mimicking bioattachment devices. Advanced Materials, 2007, 19(15): 1973–1977

62. Gorb S, Varenberg M, Peressadko A, Tuma J. Biomimetic mushroom-shaped fibrillar adhesive microstructure. Journal of the Royal Society Interface, 2007, 4(13): 271–275

63. Davies J, Haq S, Hawke T, Sargent J P. A practical approach to the development of a synthetic Gecko tape. International Journal of Adhesion and Adhesives, 2009, 29(4): 380–390

64. Lee D Y, Lee D H, Lee S G, Cho K. Hierarchical gecko-inspired nanohairs with a high aspect ratio induced by nanoyielding. Soft Matter, 2012, 8(18): 4905–4910

65. Li X S, Tao D S, Lu H, Bai P, Liu Z, Ma L, Meng Y, Tian Y. Recent developments in gecko-inspired dry adhesive surfaces from fabrication to application. Surface Topography: Metrology and Properties, 2019, 7(2): 023001

66. Murphy M P, Kim S, Sitti M. Enhanced adhesion by gecko-inspired hierarchical fibrillar adhesives. ACS Applied Materials & Interfaces, 2009, 1(4): 849–855

67. Wang Y, Hu H, Shao J Y, Ding Y C. Fabrication of well-defined mushroom-shaped structures for biomimetic dry adhesive by conventional photolithography and molding. ACS Applied Materials & Interfaces, 2014, 6(4): 2213–2218

68. Wang Y, Tian H M, Shao J Y, Sameoto D, Li X M, Wang L, Hu H, Ding Y C, Lu B H. Switchable dry adhesion with step-like micropillars and controllable interfacial contact. ACS Applied Materials & Interfaces, 2016, 8(15): 10029–10037

69. Jeong H E, Lee J K, Kim H N, Moon S H, Suh K Y. A nontransferring dry adhesive with hierarchical polymer nanohairs. Proceedings of the National Academy of Sciences of the United States of America, 2009, 106(14): 5639–5644

70. Brodoceanu D, Bauer C T, Kroner E, Arzt E, Kraus T. Hierarchical bioinspired adhesive surfaces—a review. Bioinspiration & Biomimetics, 2016, 11(5): 051001

71. Greiner C, Arzt E, del Campo A. Hierarchical gecko-like adhesives. Advanced Materials, 2009, 21(4): 479–482

72. Fischer J, Wegener M. Three-dimensional optical laser lithography beyond the diffraction limit. Laser & Photonics Reviews, 2013, 7(1): 22–44

73. Lee J, Fearing R S. Contact self-cleaning of synthetic gecko adhesive from polymer microfibers. Langmuir, 2008, 24(19): 10587–10591

74. Liu K S, Jiang L. Bio-inspired self-cleaning surfaces. Annual Review of Materials Research, 2012, 42: 231–263

75. Gillies A G, Puthoff J, Cohen M J, Autumn K, Fearing R S. Dry self-cleaning properties of hard and soft fibrillar structures. ACS Applied Materials & Interfaces, 2013, 5(13): 6081–6088

76. Mengüç Y, Röhrig M, Abusomwan U, Hölscher H, Sitti M. Staying sticky: contact self-cleaning of gecko-inspired adhesives. Journal of the Royal Society, Interface, 2014, 11(94): 20131205

77. Jagdheesh R, Diaz M, Ocana J L. Bio inspired self-cleaning ultrahydrophobic aluminium surface by laser processing. RSC

Advances, 2016, 6(77): 72933–72941

78. Bovero E, Krahn J, Menon C. Fabrication and testing of self cleaning dry adhesives utilizing hydrophobicity gradient. Journal of Bionics Engineering, 2015, 12(2): 270–275

79. Kwak M K, Jeong H E, Suh K Y. Rational design and enhanced biocompatibility of a dry adhesive medical skin patch. Advanced Materials, 2011, 23(34): 3949–3953

80. Henrey M, Ahmed A, Boscariol P, Shannon L, Menon C. Abigaille-III: a versatile, bioinspired hexapod for scaling smooth vertical surfaces. Journal of Bionics Engineering, 2014, 11(1): 1–17

81. Liu Y H, Seo T W. AnyClimb-II: dry-adhesive linkage-type climbing robot for uneven vertical surfaces. Mechanism and Machine Theory, 2018, 124: 197–210

82. Unver O, Uneri A, Aydemir A, Sitti M. Geckobot: a gecko inspired climbing robot using elastomer adhesives. In: Proceedings of 2006 IEEE International Conference on Robotics and Automation. Orlando: IEEE, 2006, 2329–2335

83. Ko H, Yi H, Jeong H E. Wall and ceiling climbing quadruped robot with superior water repellency manufactured using 3D printing (UNIclimb). International Journal of Precision Engineering and Manufacturing-Green Technology, 2017, 4(3): 273–280

84. Shao D H, Chen J, Ji A H, Dai Z D, Manoonpong P. Hybrid soft-rigid foot with dry adhesive material designed for a gecko-inspired climbing robot. In: Proceedings of 2020 the 3rd IEEE International Conference on Soft Robotics. New Haven: IEEE, 2020, 578–585

85. Birkmeyer P, Gillies A G, Fearing R S. Dynamic climbing of near-vertical smooth surfaces. In: Proceedings of 2012 IEEE/RSJ International Conference on Intelligent Robots and Systems. Vilamoura-Algarve: IEEE, 2012, 286–292

86. Li Y S, Ahmed A, Sameoto D, Menon C. Abigaille II: toward the development of a spider-inspired climbing robot. Robotica, 2012, 30(1): 79–89

87. Liu Y H, Kim H G, Seo T W. AnyClimb: a new wall-climbing robotic platform for various curvatures. IEEE/ASME Transactions on Mechatronics, 2016, 21(4): 1812–1821

88. Murphy M P, Sitti M. Waalbot: an agile small-scale wall-climbing robot utilizing dry elastomer adhesives. IEEE/ASME Transactions on Mechatronics, 2007, 12(3): 330–338

89. Lee G, Kim H, Seo K, Kim J, Sitti M, Seo T W. Series of multilinked caterpillar track-type climbing robots. Journal of Field Robotics, 2016, 33(6): 737–750

90. Murphy M P, Kute C, Mengüç Y, Sitti M. Waalbot II: adhesion recovery and improved performance of a climbing robot using fibrillar adhesives. The International Journal of Robotics Research, 2011, 30(1): 118–133

91. Dharmawan A G, Xavier P, Hariri H H, Soh G S, Baji A, Bouffanais R, Foong S H, Low H Y, Wood K L. Design, modeling, and experimentation of a bio-inspired miniature climbing robot with bilayer dry adhesives. Journal of Mechanisms and Robotics, 2019, 11(2): 020902

92. Unver O, Sitti M. Tankbot: a palm-size, tank-like climbing robot using soft elastomer adhesive treads. The International Journal of Robotics Research, 2010, 29(14): 1761–1777

93. Song S, Drotlef D M, Majidi C, Sitti M. Controllable load sharing for soft adhesive interfaces on three-dimensional surfaces. Proceedings of the National Academy of Sciences of the United States of America, 2017, 114(22): E4344–E4353

94. Glick P, Suresh S A, Ruffatto D, Cutkosky M, Tolley M T, Parness A. A soft robotic gripper with gecko-inspired adhesive. IEEE Robotics and Automation Letters, 2018, 3(2): 903–910

95. Hashizume J, Huh T M, Suresh S A, Cutkosky M R. Capacitive sensing for a gripper with gecko-inspired adhesive film. IEEE Robotics and Automation Letters, 2019, 4(2): 677–683

96. Ruotolo W, Brouwer D, Cutkosky M R. From grasping to manipulation with gecko-inspired adhesives on a multifinger gripper. Science Robotics, 2021, 6(61): eabi9773

97. Dadkhah M, Zhao Z Y, Wettels N, Spenko M. A self-aligning gripper using an electrostatic/gecko-like adhesive. In: Proceeding of 2016 IEEE/RSJ International Conference on Intelligent Robots and Systems. Daejeon: IEEE, 2016, 1006–1011

98. Hawkes E W, Jiang H, Cutkosky M R. Three-dimensional dynamic surface grasping with dry adhesion. The International Journal of Robotics Research, 2016, 35(8): 943–958

99. Hao Y F, Biswas S, Hawkes E W, Wang T M, Zhu M J, Wen L, Visell Y. A multimodal, enveloping soft gripper: shape conformation, bioinspired adhesion, and expansion-driven suction. IEEE Transactions on Robotics, 2021, 37(2): 350–362

100. Hu Q Q, Dong E B, Sun D. Soft gripper design based on the integration of flat dry adhesive, soft actuator, and microspine. IEEE Transactions on Robotics, 2021, 37(4): 1065–1080

101. Niederegger S, Gorb S. Tarsal movements in flies during leg attachment and detachment on a smooth substrate. Journal of Insect Physiology, 2003, 49(6): 611–620

102. Persson B N J. Wet adhesion with application to tree frog adhesive toe pads and tires. Journal of Physics Condensed Matter, 2007, 19(37): 376110

103. Scholz I, Barnes W J P, Smith J M, Baumgartner W. Ultrastructure and physical properties of an adhesive surface, the toe pad epithelium of the tree frog, Litoria caerulea White. Journal of Experimental Biology, 2009, 212(2): 155–162

104. He B, Wang Z B, Li M H, Wang K, Shen R J, Hu S Q. Wet adhesion inspired bionic climbing robot. IEEE/ASME Transactions on Mechatronics, 2014, 19(1): 312–320

105. Labonte D and Federle W. Scaling and biomechanics of surface attachment in climbing animals. Philosophical Transactions of the Royal Society B: Biological Sciences, 2015, 370(1661): 20140027

106. Slater D M, Vogel M J, Macner A M, Steen P H. Beetle-inspired adhesion by capillary-bridge arrays: pull-off detachment. Journal of Adhesion Science and Technology, 2014, 28(3–4): 273–289

107. De Souza E J, Brinkmann M, Mohrdieck C, Arzt E. Enhancement of capillary forces by multiple liquid bridges. Langmuir, 2008, 24(16): 8813–8820

108. Crawford N, Endlein T, Barnes W J P. Self-cleaning in tree frog toe pads; a mechanism for recovering from contamination without the need for grooming. Journal of Experimental Biology, 2012, 215(22): 3965–3972

109. Tulchinsky A, Gat A D. Viscous-poroelastic interaction as mechanism to create adhesion in frogs' toe pads. Journal of Fluid

Mechanics, 2015, 775: 288–303

110. Chen Y P, Meng J X, Gu Z, Wan X Z, Jiang L, Wang S T. Bioinspired multiscale wet adhesive surfaces: structures and controlled adhesion. Advanced Functional Materials, 2020, 30(5): 1905287

111. Zhang C, Wu B H, Zhou Y S, Zhou F, Liu W M, Wang Z K. Mussel-inspired hydrogels: from design principles to promising applications. Chemical Society Reviews, 2020, 49(11): 3605–3637

112. Sedó J, Saiz-Poseu J, Busqué F, Ruiz-Molina D. Catechol-based biomimetic functional materials. Advanced Materials, 2013, 25(5): 653–701

113. Huang J W, Liu Y, Yang Y X, Zhou Z J, Mao J, Wu T, Cai Q P, Peng C H, Xu Y T, Zeng B R, Luo W A, Chen G R, Yuan C H, Dai L Z. Electrically programmable adhesive hydrogels for climbing robots. Science Robotics, 2021, 6(53): eabe1858

114. Chen H W, Zhang L W, Zhang D Y, Zhang P F, Han Z W. Bioinspired surface for surgical graspers based on the strong wet friction of tree frog toe pads. ACS Applied Materials & Interfaces, 2015, 7(25): 13987–13995

115. Ko H, Seong M, Jeong H E. A micropatterned elastomeric surface with enhanced frictional properties under wet conditions and its application. Soft Matter, 2017, 13(45): 8419–8425

116. Vogel M J, Steen P H. Capillarity-based switchable adhesion. Proceedings of the National Academy of Sciences of the United States of America, 2010, 107(8): 3377–3381

117. Meng F D, Liu Q, Wang X, Tan D, Xue L J, Barnes W J P. Tree frog adhesion biomimetics: opportunities for the development of new, smart adhesives that adhere under wet conditions. Philosophical Transactions of the Royal Society A: Mathematical, Physical, and Engineering Sciences, 2019, 377(2150): 20190131

118. Iturri J, Xue L J, Kappl M, García-Fernández L, Barnes W J P, Butt H J, del Campo A. Torrent frog-inspired adhesives: attachment to flooded surfaces. Advanced Functional Materials, 2015, 25(10): 1499–1505

119. Xie J, Li M, Dai Q W, Huang W, Wang X L. Key parameters of biomimetic patterned surface for wet adhesion. International Journal of Adhesion and Adhesives, 2018, 82: 72–78

120. Xue L J, Sanz B, Luo A Y, Turner K T, Wang X, Tan D, Zhang R, Du H, Steinhart M, Mijangos C, Guttmann M, Kappl M, del Campo A. Hybrid surface patterns mimicking the design of the adhesive toe pad of tree frog. ACS Nano, 2017, 11(10): 9711–9719

121. Drotlef D M, Stepien L, Kappl M, Barnes W J P, Butt H J, del Campo A. Insights into the adhesive mechanisms of tree frogs using artificial mimics. Advanced Functional Materials, 2013, 23(9): 1137–1146

122. Chen Y F, Doshi N, Wood R J. Inverted and inclined climbing using capillary adhesion in a quadrupedal insect-scale robot. IEEE Robotics and Automation Letters, 2020, 5(3): 4820–4827

123. Lee B P. Climbing robots in a sticky situation. Science Robotics, 2021, 6(53): eabh2682

124. Van Nguyen P, Ho V A. Grasping interface with wet adhesion and patterned morphology: case of thin shell. IEEE Robotics and Automation Letters, 2019, 4(2): 792–799

125. Suzuki K, Nemoto S, Fukuda T, Takanobu H, Miura H. Insect-

inspired wall-climbing robots utilizing surface tension forces. Journal of Advanced Mechanical Design, Systems, and Manufacturing, 2010, 4(1): 383–390

126. Li M H, He B, Qin H Y, Zhou Y M, Lu H X, Yue J G. A wet adhesion inspired biomimetic pad with direction dependence and adaptability. Chinese Science Bulletin, 2011, 56(18): 1935–1941

127. Xin W C, Pan F T L, Li Y H, Chiu P W Y, Li Z. Design and modeling of a biomimetic gastropod-like soft robot with wet adhesive locomotion. In: Proceedings of 2021 IEEE International Conference on Robotics and Automation. Xi'an: IEEE, 2021, 11997–12003

128. Van Nguyen P, Luu Q K, Takamura Y, Ho V A. Wet adhesion of micro-patterned interfaces for stable grasping of deformable objects. In: Proceedings of 2020 IEEE/RSJ International Conference on Intelligent Robots and Systems. Las Vegas: IEEE, 2020, 9213–9219

129. Roderick W R, Chin D D, Cutkosky M R, Lentink D. Birds land reliably on complex surfaces by adapting their foot-surface interactions upon contact. eLife, 2019, 8: e46415

130. Zani P A. The comparative evolution of lizard claw and toe morphology and clinging performance. Journal of Evolutionary Biology, 2000, 13(2): 316–325

131. Spenko M, Cutkosky M, Majidi C, Fearing R, Groff R, Autumn K. Foot design and integration for bioinspired climbing robots. In: Gerhart G R, Shoemaker C M, Gage D W, eds. Unmanned Systems Technology VIII. Bellingham: SPIE, 2006, 623019

132. Lam T L, Xu Y S. Biologically inspired tree-climbing robot with continuum maneuvering mechanism. Journal of Field Robotics, 2012, 29(6): 843–860

133. Sarmiento-Ponce E J, Sutcliffe M P F, Hedwig B. Substrate texture affects female cricket walking response to male calling song. Royal Society Open Science, 2018, 5(3): 172334

134. Frantsevich L, Gorb S. Structure and mechanics of the tarsal chain in the hornet, Vespa crabro (Hymenoptera: Vespidae): implications on the attachment mechanism. Arthropod Structure & Development, 2004, 33(1): 77–89

135. Woodward M A, Sitti M. Morphological intelligence counters foot slipping in the desert locust and dynamic robots. Proceedings of the National Academy of Sciences of the United States of America, 2018, 115(36): E8358–E8367

136. Han L B, Wang Z Y, Ji A H, Dai Z D. Grip and detachment of locusts on inverted sandpaper substrates. Bioinspiration & Biomimetics, 2011, 6(4): 046005

137. Roderick W R, Cutkosky M R, Lentink D. Bird-inspired dynamic grasping and perching in arboreal environments. Science Robotics, 2021, 6(61): eabj7562

138. Pattrick J G, Labonte D, Federle W. Scaling of claw sharpness: mechanical constraints reduce attachment performance in larger insects. Journal of Experimental Biology, 2018, 221(24): jeb188391

139. Asbeck A T, Kim S, Cutkosky M R, Provancher W R, Lanzetta M. Scaling hard vertical surfaces with compliant microspine arrays. The International Journal of Robotics Research, 2006, 25(12): 1165–1179

140. Lee J S, Plecnik M, Yang J H, Fearing R S. Self-engaging spined gripper with dynamic penetration and release for steep jumps. In:

Proceedings of 2018 IEEE international conference on robotics and automation. Brisbane: IEEE, 2018, 6082–6089

141. Liu Y W, Sun S M, Wu X, Mei T. A wheeled wall-climbing robot with bio-inspired spine mechanisms. Journal of Bionics Engineering, 2015, 12(1): 17–28

142. Wang S Q, Jiang H, Cutkosky M R. Design and modeling of linearly-constrained compliant spines for human-scale locomotion on rocky surfaces. The International Journal of Robotics Research, 2017, 36(9): 985–999

143. Sintov A, Avramovich T, Shapiro A. Design and motion planning of an autonomous climbing robot with claws. Robotics and Autonomous Systems, 2011, 59(11): 1008–1019

144. Brown J M, Austin M P, Miller B D, Clark J E. Evidence for multiple dynamic climbing gait families. Bioinspiration & Biomimetics, 2019, 14(3): 036001

145. Weiss L E, Merz R, Prinz F B, Neplotnik G, Padmanabhan P, Schultz L, Ramaswami K. Shape deposition manufacturing of heterogeneous structures. Journal of Manufacturing Systems, 1997, 16(4): 239–248

146. Lynch G A, Clark J E, Lin P C, Koditschek D E. A bioinspired dynamical vertical climbing robot. The International Journal of Robotics Research, 2012, 31(8): 974–996

147. Hu Q Q, Dong E B, Cheng G, Jin H, Yang J, Sun D. Inchworm-inspired soft climbing robot using microspine arrays. In: Proceedings of 2019 IEEE/RSJ International Conference on Intelligent Robots and Systems. Macao: IEEE, 2019, 5800–5805

148. Liu Y W, Wang L M, Niu F Z, Li P Y, Li Y, Mei T. A track-type inverted climbing robot with bio-inspired spiny grippers. Journal of Bionics Engineering, 2020, 17(5): 920–931

149. Carpenter K, Wiltsie N, Parness A. Rotary microspine rough surface mobility. IEEE/ASME Transactions on Mechatronics, 2016, 21(5): 2378–2390

150. Backus S B, Onishi R, Bocklund A, Berg A, Contreras E D, Parness A. Design and testing of the JPL-Nautilus gripper for deep-ocean geological sampling. Journal of Field Robotics, 2020, 37(6): 972–986

151. Xu F Y, Wang B, Shen J J, Hu J L, Jiang G P. Design and realization of the claw gripper system of a climbing robot. Journal of Intelligent & Robotic Systems, 2018, 89(3): 301–317

152. Su M J, Guan Y S, Huang D Y, Zhu H F. Modeling and analysis of a passively adaptive soft gripper with the bio-inspired compliant mechanism. Bioinspiration & Biomimetics, 2021, 16(5): 055001

153. Uckert K, Parness A, Chanover N, Eshelman E J, Abcouwer N, Nash J, Detry R, Fuller C, Voelz D, Hull R, Flannery D, Bhartia R, Manatt K S, Abbey W J, Boston P. Investigating habitability with an integrated rock-climbing robot and astrobiology instrument suite. Astrobiology, 2020, 20(12): 1427–1449

154. Kwasi Boohene A N, Newill-Smith D, Trieu T, Stengel R F. Prototype for an asteroid exploratory robot using multi-phalanx microspine grippers. In: Proceedings of AIAA SPACE Conference and Exposition. Reston: AIAA, 2015, 4585

155. Nagaoka K, Minote H, Maruya K, Shirai Y, Yoshida K, Hakamada T, Sawada H, Kubota T. Passive spine gripper for free-climbing robot in extreme terrain. IEEE Robotics and Automation Letters, 2018, 3(3): 1765–1770

156. Uno K, Takada N, Okawara T, Haji K, Candalot A, Ribeiro W F R, Nagaoka K, Yoshida K. Hubrobo: a lightweight multi-limbed climbing robot for exploration in challenging terrain. In: Proceedings of 2020 IEEE-RAS the 20th International Conference on Humanoid Robots (Humanoids). Munich: IEEE, 2021, 209–215

157. Jiang H, Wang S Q, Cutkosky M R. Stochastic models of compliant spine arrays for rough surface grasping. The International Journal of Robotics Research, 2018, 37(7): 669–687

158. Wang S Q, Jiang H, Myung Huh T, Sun D N, Ruotolo W, Miller M, Roderick W R T, Stuart H S, Cutkosky M R. Spinyhand: contact load sharing for a human-scale climbing robot. Journal of Mechanisms and Robotics, 2019, 11(3): 031009

159. Ruotolo W, Roig F S, Cutkosky M R. Load-sharing in soft and spiny paws for a large climbing robot. IEEE Robotics and Automation Letters, 2019, 4(2): 1439–1446

160. Xu F Y, Meng F C, Jiang Q S, Peng G L. Grappling claws for a robot to climb rough wall surfaces: mechanical design, grasping algorithm, and experiments. Robotics and Autonomous Systems, 2020, 128: 103501

161. Tavakoli M, Marjovi A, Marques L, de Almeida A T. 3DCLIMBER: a climbing robot for inspection of 3D human made structures. In: Proceedings of 2008 IEEE/RSJ International Conference on Intelligent Robots and Systems. Nice: IEEE, 2008, 4130–4135

162. Guan Y S, Jiang L, Zhu H F, Wu W Q, Zhou X F, Zhang H, Zhang X M. Climbot: a bio-inspired modular biped climbing robot—system development, climbing gaits, and experiments. Journal of Mechanisms and Robotics, 2016, 8(2): 021026

163. Liu Y Y, Lam T L, Qian H H, Xu Y S. Design and analysis of gripper with retractable spine for tree climbing robots. In: Proceedings of 2014 IEEE International Conference on Information and Automation. Hailar: IEEE, 2014, 350–355

164. Tramacere F, Beccai L, Sinibaldi E, Laschi C, Mazzolai B. Adhesion mechanisms inspired by octopus suckers. Procedia Computer Science, 2011, 7: 192–193

165. Kier W M, Smith A M. The morphology and mechanics of octopus suckers. Biological Bulletin, 1990, 178(2): 126–136

166. Kier W M, Smith A M. The structure and adhesive mechanism of octopus suckers. Integrative and Comparative Biology, 2002, 42(6): 1146–1153

167. Tramacere F, Beccai L, Mattioli F, Sinibaldi E, Mazzolai B. Artificial adhesion mechanisms inspired by octopus suckers. In: Proceedings of 2012 IEEE International Conference on Robotics and Automation. Saint Paul: IEEE, 2012, 3846–3851

168. Tramacere F, Pugno N M, Kuba M J, Mazzolai B. Unveiling the morphology of the acetabulum in octopus suckers and its role in attachment. Interface Focus, 2015, 5(1): 20140050

169. Weihs D, Fish F E, Nicastro A J. Mechanics of remora removal by dolphin spinning. Marine Mammal Science, 2007, 23(3): 707–714

170. Gamel K M, Garner A M, Flammang B E. Bioinspired remora adhesive disc offers insight into evolution. Bioinspiration & Biomimetics, 2019, 14(5): 056014

171. Beckert M, Flammang B E, Nadler J H. Remora fish suction pad attachment is enhanced by spinule friction. Journal of

Experimental Biology, 2015, 218(22): 3551–3558

172. Wang S Q, Li L, Chen Y F, Kenaley C, Wainwright D, Wood R J, Wen L. The detachment of remora: kinematics, dynamics, and a bio-robotic model. In: Proceedings of Annual Meeting of Society of Integrative Orgasmic Biology. Tampa: Society for Integrative and Comparative Biology, 2019, 59: E241–E241

173. Fulcher B A, Motta P J. Suction disk performance of echeneid fishes. Canadian Journal of Zoology, 2006, 84(1): 42–50

174. Wang S Q, Li L, Chen Y F, Wang Y P, Sun W G, Xiao J F, Wainwright D. Wang T M, Wood R J, Wen L. A bio-robotic remora disc with attachment and detachment capabilities for reversible underwater hitchhiking. In: Proceedings of 2019 IEEE International Conference on Robotics and Automation. New York: IEEE, 2019, 4653–4659

175. Ditsche P, Wainwright D K, Summers A P. Attachment to challenging substrates-fouling, roughness and limits of adhesion in the northern clingfish (Gobiesox maeandricus). Journal of Experimental Biology, 2014, 217(14): 2548–2554

176. Wainwright D K, Kleinteich T, Kleinteich A, Gorb S N, Summers A P. Stick tight: suction adhesion on irregular surfaces in the northern clingfish. Biology Letters, 2013, 9(3): 20130234

177. Ditsche P, Summers A. Learning from northern clingfish (Gobiesox maeandricus): bioinspired suction cups attach to rough surfaces. Philosophical Transactions of the Royal Society B: Biological Sciences, 2019, 374(1784): 20190204

178. Wang J R, Ji C, Wang W, Zou J, Yang H Y, Pan M. An adhesive locomotion model for the rock-climbing fish, beaufortia kweichowensis. Scientific Reports, 2019, 9(1): 16571

179. Kim S, Asbeck A T, Cutkosky M R, Provancher W R. SpinybotII: climbing hard walls with compliant microspines. In: Proceedings of the 12th International Conference on Advanced Robotics (ICAR'05). Seattle: IEEE, 2005, 601–606

180. Gerstner C L. Effect of oral suction and other friction-enhancing behaviors on the station-holding performance of suckermouth catfish (Hypostomus spp.). Canadian Journal of Zoology, 2007, 85(1): 133–140

181. Follador M, Tramacere F, Mazzolai B. Dielectric elastomer actuators for octopus inspired suction cups. Bioinspiration & Biomimetics, 2014, 9(4): 046002

182. Hu B S, Wang L W, Fu Z, Zhao Y Z. Bio-inspired miniature suction cups actuated by shape memory alloy. International Journal of Advanced Robotic Systems, 2009, 6(3): 151–160

183. Wang S H, Luo H Y, Linghu C H, Song J Z. Elastic energy storage enabled magnetically actuated, octopus-inspired smart adhesive. Advanced Functional Materials, 2021, 31(9): 2009217

184. Mazzolai B, Mondini A, Tramacere F, Riccomi G, Sadeghi A, Giordano G, Del Dottore E, Scaccia M, Zampato M, Carminati S. Octopus-inspired soft arm with suction cups for enhanced grasping tasks in confined environments. Advanced Intelligent Systems, 2019, 1(6): 1900041

185. Tang Y C, Zhang Q T, Lin G J, Yin J. Switchable adhesion actuator for amphibious climbing soft robot. Soft Robotics, 2018, 5(5): 592–600

186. Sholl N, Moss A, Kier W M, Mohseni K. A soft end effector inspired by cephalopod suckers and augmented by a dielectric elastomer actuator. Soft Robotics, 2019, 6(3): 356–367

187. Xie Z X, Domel A G, An N, Green C, Gong Z Y, Wang T M, Knubben E M, Weaver J C, Bertoldi K, Wen L. Octopus arm-inspired tapered soft actuators with suckers for improved grasping. Soft Robotics, 2020, 7(5): 639–648

188. Asbeck A, Dastoor S, Parness A, Fullerton L, Esparza N, Soto D, Heyneman B, Cutkosky M. Climbing rough vertical surfaces with hierarchical directional adhesion. In: Proceedings of 2009 IEEE International Conference on Robotics and Automation. Kobe: IEEE, 2009, 2675–2680

189. Patil S, Mangal R, Malasi A, Sharma A. Biomimetic wet adhesion of viscoelastic liquid films anchored on micropatterned elastic substrates. Langmuir, 2012, 28(41): 14784–14791

190. Lee H, Lee B P, Messersmith P B. A reversible wet/dry adhesive inspired by mussels and geckos. Nature, 2007, 448(7151): 338–341

191. Liu J F, Xu L S, Chen S Q, Xu H, Cheng G X, Xu J J. Development of a bio-inspired wall-climbing robot composed of spine wheels, adhesive belts and eddy suction cup. Robotica, 2021, 39(1): 3–22

192. Daltorio K A, Wei T E, Gorb S N, Ritzmann R E, Quinn R D. Passive foot design and contact area analysis for climbing mini-whegs. In: Proceedings of 2007 IEEE International Conference on Robotics and Automation. Rome: IEEE, 2007, 1274–1279

193. Wang B C, Xiong X F, Duan J J, Wang Z Y, Dai Z D. Compliant detachment of wall-climbing robot unaffected by adhesion state. Applied Sciences, 2021, 11(13): 5860

194. Provancher W R, Jensen-Segal S I, Fehlberg M A. ROCR: an energy-efficient dynamic wall-climbing robot. IEEE/ASME Transactions on Mechatronics, 2011, 16(5): 897–906

195. Austin M P, Brown J M, Young C A, Clark J E. Leg design to enable dynamic running and climbing on BOBCAT. In: Proceedings of 2018 IEEE/RSJ International Conference on Intelligent Robots and Systems. Madrid: IEEE, 2018, 3799–3806

196. Cutkosky M R. Climbing with adhesion: from bioinspiration to biounderstanding. Interface Focus, 2015, 5(4): 20150015

197. Ji A H, Zhao Z H, Manoonpong P, Wang W, Chen G M, Dai Z D. A bio-inspired climbing robot with flexible pads and claws. Journal of Bionics Engineering, 2018, 15(2): 368–378

198. Bian S Y, Wei Y L, Xu F, Kong D Y. A four-legged wall-climbing robot with spines and miniature setae array inspired by Longicorn and Gecko. Journal of Bionics Engineering, 2021, 18(2): 292–305

199. Goldman D I, Chen T S, Dudek D M, Full R J. Dynamics of rapid vertical climbing in cockroaches reveals a template. Journal of Experimental Biology, 2006, 209(15): 2990–3000

200. Raibert M, Chepponis M, Brown H. Running on four legs as though they were one. IEEE Journal on Robotics and Automation, 1986, 2(2): 70–82

201. Hutter M, Sommer H, Gehring C, Hoepflinger M, Bloesch M, Siegwart R. Quadrupedal locomotion using hierarchical operational space control. The International Journal of Robotics Research, 2014, 33(8): 1047–1062

202. Haomachai W, Shao D H, Wang W, Ji A H, Dai Z D, Manoonpong P. Lateral undulation of the bendable body of a gecko-inspired robot for energy-efficient inclined surface climbing. IEEE Robotics and Automation Letters, 2021, 6(4):

7917–7924

203. Yang G Z, Bellingham J, Dupont P E, Fischer P, Floridi L, Full R, Jacobstein N, Kumar V, McNutt M, Merrifield R, Nelson B J, Scassellati B, Taddeo M, Taylor R, Veloso M, Wang Z L, Wood R. The grand challenges of *Science Robotics*. Science Robotics, 2018, 3(14): eaar7650

204. Zhang P F, Wu Z X, Meng Y, Dong H J, Tan M, Yu J Z. Development and control of a bioinspired robotic remora for hitchhiking. IEEE/ASME Transactions on Mechatronics, 2021 (in press)

205. Liu H X, Huang Q, Zhang W M, Chen X C, Yu Z G, Meng L B, Bao L, Ming A G, Huang Y, Hashimoto K, Takanishi A. Cat-inspired mechanical design of self-adaptive toes for a legged robot. In: Proceedings of 2016 IEEE/RSJ International Conference on Intelligent Robots and Systems. Daejeon: IEEE, 2016, 2425–2430